



**HAL**  
open science

## Observing G4 formation and its resolution by Pif1 in real time by manipulation under magnetic tweezers

Jessica Valle-Orero, Martin Rieu, Jean-François Allemand, Dulamkhuu Bujaa, Alexandra Joubert, Phong Lan Thao Tran, Vincent Croquette, Jean-Baptiste Boulé

### ► To cite this version:

Jessica Valle-Orero, Martin Rieu, Jean-François Allemand, Dulamkhuu Bujaa, Alexandra Joubert, et al.. Observing G4 formation and its resolution by Pif1 in real time by manipulation under magnetic tweezers. Kevin D. Raney; Robert L. Eoff; Alicia K. Byrd; Samantha Kendrick. G4 and i-motif biology, 695, Elsevier, pp.119-158, 2024, Methods in Enzymology, 10.1016/bs.mie.2023.12.012 . hal-04664921

**HAL Id: hal-04664921**

**<https://hal.science/hal-04664921v1>**

Submitted on 30 Jul 2024

**HAL** is a multi-disciplinary open access archive for the deposit and dissemination of scientific research documents, whether they are published or not. The documents may come from teaching and research institutions in France or abroad, or from public or private research centers.

L'archive ouverte pluridisciplinaire **HAL**, est destinée au dépôt et à la diffusion de documents scientifiques de niveau recherche, publiés ou non, émanant des établissements d'enseignement et de recherche français ou étrangers, des laboratoires publics ou privés.

# Observing G4 formation and its resolution by Pif1 in real time by manipulation under magnetic tweezers

Jessica Valle-Orero<sup>1,2,3,\*</sup>, Martin Rieu<sup>1,2,4</sup>, Jean-François Allemand<sup>1,2</sup>, Dulamkhuu Bujaa<sup>1,2</sup>,  
Alexandra Joubert<sup>5</sup>, Phong Lan Thao Tran<sup>5,6</sup>, Vincent Croquette<sup>1,2,7,\*</sup>, and  
Jean-Baptiste Boulé<sup>5\*\*</sup>

September 2023

## Contents

<b>1</b>	<b>Introduction</b>	<b>2</b>
<b>2</b>	<b>Formation and Observation of G4 structure in a double-stranded context</b>	<b>3</b>
2.1	Construction of a DNA hairpin containing a G4 sequence . . . . .	4
2.1.1	Long DNA hairpin with a G4 embedded . . . . .	4
2.1.2	Small DNA hairpins with a G4 sequence embedded . . . . .	7
2.2	Bead preparation . . . . .	9
2.3	Single-molecule measurements : the stability and folding rate of G-quadruplexes. . .	10
2.3.1	Orientation . . . . .	13
2.4	Quantitative analysis of folding and unfolding dynamics of G4 structures . . . . .	13
<b>3</b>	<b>Observation of Helicase activity in a DNA hairpin</b>	<b>15</b>
3.1	Pif1 helicase expression and purification . . . . .	16
3.2	Force-dependent helicase . . . . .	18
3.3	Pif1 unwinding and G4 Resolvase activity . . . . .	19
3.3.1	Pif1 unwinds the double-stranded hairpin . . . . .	20
3.3.2	Pif1 interacts with G4 in the lagging strand . . . . .	20
3.3.3	Pif1 interacts with G4 in the leading strand . . . . .	21
3.3.4	Pif1 resolves G4 [Valle-Orero et al., 2022] . . . . .	21
3.3.5	Kinetics of Pif1 binding to DNA substrates . . . . .	22
<b>4</b>	<b>Discussion</b>	<b>24</b>
<b>5</b>	<b>Funding</b>	<b>24</b>

---

\*To whom correspondence should be addressed. Tel: +33 140795616; Fax: +33 1407937050; Email: jean-baptiste.boule@mnhn.fr. Correspondence may also be addressed to Vincent Croquette. Email: vincent.croquette@espci.psl.eu, and Jessica Valle-Orero. Email: jvalleorero@aup.edu

## Abstract

G-quadruplexes are nucleic acids secondary structures that may form in guanine-rich sequences, either intra or inter-molecularly. Ability of a primary sequence to form a G4 can be predicted computationally with an improving accuracy as well as tested in bulk using biophysical measurements. As a result, G4 density maps have been devised for a large number of genomes from all life kingdoms. Experimental validation of the formation of G-quadruplexes in vivo however remains indirect and relies on small molecule, antibody or protein stabilization to measure downstream effects on gene expression or genome stability for example. Although numerous techniques exist to observe spontaneous formation of G-quadruplexes in single-stranded DNA, observing G4 formation in double-stranded DNA is more challenging. However, it is particularly relevant to understand if a given G4 sequence forms stably in a dsDNA context, if it is stable enough to dock proteins or pose a challenge to molecular motors such as helicases or polymerases. In essence, G4s can be a threat to genomic stability but carry as well the potential to be elements of a structural language in the non-replicating genome. To study quantitatively the formation dynamics and stability of single intramolecular G4s embedded in dsDNA, we have adapted techniques of DNA manipulation under magnetic tweezers. This technique serves also for the basis of studying encounters of molecular motors with G4 at a single molecule resolution, in order to gain insight into the specificity of G4 resolution by molecular motors, and its efficiency. The procedures described here include the design of the G4 substrate, the study of G4 formation probability and lifetime in double-stranded DNA, as well as procedures to study the encounter between the Pif1 helicase and a G4 until G4 resolution. The procedures that we described here can easily be extended to the study of other G4s or molecular motors.

## 1 Introduction

G-quadruplexes (G4s) are non-conventional nucleic acid secondary structures that may form in G-rich DNA or RNA molecules. These structures are characterized by the stacking of coplanar guanine quartets (G-quartets), with 2 or more guanines in each quartet interacting via Hoogsteen hydrogen bonds. Stabilized by monovalent cations, such as  $K^+$  or  $Na^+$ , G4 may form intra- or inter-molecular structures, and adapt different folding patterns (parallel, antiparallel, or mixed). These sequences are widespread across all genomes, albeit at variable density. Depending on the sequence and physiological conditions, G4 structures of different folding patterns can potentially form across the genome and are shown to interfere with or promote multiple nucleic acid transactions, including DNA replication, gene expression, mRNA translation, DNA repair, or telomere maintenance. When they form in DNA, G4-forming sequences are generally surrounded by double-stranded (ds) DNA regions, for example in promoters [Siddiqui-Jain et al., 2002], minisatellites [Ribeyre et al., 2009], or replication origins [Valton et al., 2014]. These double-stranded G4s, if they are stable and unprocessed by helicases, have the potential to pose significant challenges during DNA replication and transcription, impeding the progression of the replication fork or the transcription bubble [Mendoza et al., 2016, Lerner and Sale, 2019, Paeschke et al., 2013]. This can result in fork pausing, where the replication process temporarily halts, or can promote DNA breakage, with detrimental consequences for genomic stability.

Interestingly, despite G4 being potential roadblocks for molecular motors, current scientific understanding suggests that evolution has preserved these sequences over time [Paeschke et al., 2011, Bugaut and Balasubramanian, 2012, Bohálová et al., 2021, Capra et al., 2010]. This evolutionary conservation hints at a possible role for G4 in encoding structural information within DNA. This structural information is expected to originate from the ability of the G-rich sequence to form G4

when the DNA sequence is in ssDNA form (at telomeres for example), in a dsDNA context (promoters, immunoglobulin genes) or in RNA following transcription. Moreover, the ability of a G4 to form stable structure can be affected by nucleotide modification, either on the G4 forming sequence itself (e.g. guanine oxidation into oxoguanines) or on the opposite strand (e.g. methylation of cytosines), expanding the possibilities of the regulation of G4 formation, stabilization and recognition within the cell [Fleming et al., 2017].

During the last 30 years, many proteins with a binding ability to G4 were identified. Among the enzymes that may destabilize the G4s, helicases have emerged as essential players in the dynamic landscape of G4s. These enzymes possess the ability to unwind the double-strand DNA and for at least some of them to resolve G4 structures within this context, thereby ensuring the smooth progression of DNA replication, transcription and repair, that could be otherwise blocked by the G4. The interplay between G4 structures and helicases has garnered significant attention in molecular biology, as it underpins fundamental mechanisms governing genome stability and gene regulation.

In the last decades, numerous studies *in vitro* and *in vivo* have been focusing around the physiological conditions that drive the formation of G4 structures, and how these are responsible for different biological roles. Furthermore, owing to their strategic localization within the genome, the quest for identifying and characterizing the nuanced associations between G4 structures and helicases has persisted. Single molecule micromanipulation techniques are useful approaches to solve several questions about the formation of G4, their stability and their interaction with molecular motors, at the single molecule level. In particular, single molecule techniques like DNA manipulation under magnetic tweezers allow to investigate the probability of formation of a G4 within a ssDNA or dsDNA molecule, the lifetime of single G4 formation events or their fate when they encounter a molecular motor.

We have decided to work mostly on G4 structures embedded in a double-stranded DNA (dsDNA) structure which corresponds to a large set of *in vivo* situations. This type of substrate is meant to mimic a dsDNA fork that occur during replication or at a gene promoter during transcription. Here, we describe new protocols designed to investigate the folding and stability of G4 structures in dsDNA regions when embedded in a DNA hairpin. Moreover, double-stranded templates are also extremely appropriate to observe directly the activity of a helicase since we can monitor the change of extension while a helicase translocates along the double-stranded hairpin. Using these new assays we are able to further address the mechanism of G4 resolution by helicases such as Pif1 [Ribeyre et al., 2009, Paeschke et al., 2013], but can be expanded to the study of other G4s, motors, or the effect of nucleotide modification on G4 folding ability and lifetime.

This article serves as a follow-up of a previous Methodology paper focus on DNA/RNA hairpins studied using Magnetic tweezers [Tran et al., 2021]. Here, we provide a thorough methodology on synthesis of DNA hairpins, the progress made in the observation and analysis of G4 structures in single-molecule assay, the study of helicase dynamics, as well as furnishing in-detailed magnetic tweezers force protocols and the procedures used for data analysis.

## 2 Formation and Observation of G4 structure in a double-stranded context

Until now, our understanding of the conditions surrounding G4 formation has primarily been derived from *in vitro* biophysical examinations of various models G4-forming single-stranded sequences. Recent investigations utilizing magnetic or optical tweezers have focused on the folding/unfolding dynamics of several G4 structures, including those found in human telomeric or cMYC promoter sequences [Mitra et al., 2019, You et al., 2015, You et al., 2014, Yu et al., 2009, Cheng et al., 2019,

Allshire et al., 1989, Mendez-Bermudez et al., 2009, Gabelica et al., 2007]. However, most of these studies have concentrated on the dynamics of G4 in a ssDNA context. To address this, we have developed a single-molecule assay suitable for magnetic tweezers that enables the incorporation of a G4 structure within a dsDNA molecule, effectively simulating a dsDNA fork. This approach is designed to mimic structures that may occur during cellular replication or at a gene promoter [Siddiqui-Jain et al., 2002, Valton et al., 2014]. A G4 sequence embedded in a dsDNA template encounters a folding issue: as long as the double-stranded structure is maintained the G4 cannot fold. In order to fold it, one needs to unzip the double-stranded structure so that the molecule is turned in single-stranded form. To achieve this, we use a hairpin molecule structure formed of a double-stranded stem ending at one end by a small loop where nucleotides are not self-complementary while the second end is formed by a Y-shape with two stretches of non-complementary sequences. We use these two single-stranded handles to bind the molecule to a magnetic bead and to the glass surface of the cell. In a magnetic tweezers experiment we can apply stable forces (2-25 pN) to the hairpin handles. Below 15 pN (the exact force will depend on the salt concentration) the hairpin stays closed due to the hybridization interactions, but above that force, the hairpin opens until the entire molecule is in single-stranded form. Opening the hairpin is crucial to allow the G4 sequence to fold. However, at forces greater than 15 pN, the folding of G4 is severely hindered. This is because the intermediate folding of loops near the G stretch, which is necessary for nucleating the G4, becomes more challenging. If we decrease the force applied, we help form the G4 structure but we also favor the hairpin refolding, which competes efficiently with the G4 folding. For that reason, we describe the method that we have developed to hinder the hairpin refolding while allowing the G4 structure to fold. Owing to our ability to form these structures, we have been able to study the folding and persistence times of different G4 structures in a hairpin context. This section details the protocols supporting the results of our previously published studies [Tran et al., 2021, Valle-Orero et al., 2022]

## 2.1 Construction of a DNA hairpin containing a G4 sequence

The DNA substrate that we design for our single molecule experiments all contain :

- The desired G4 sequence
- A neutral sequence of dsDNA around it. The length will be adjusted as a function of processivity of the helicase to be studied: the protein should be able to reach the G4 before detaching from the molecule. This dsDNA region should however be long enough to provide dsDNA stability even if the G4 is folded.
- A loop at the apex of the hairpin which size will control the refolding force and kinetics of the hairpin [Ding et al., 2012]. The longer the loop, the lowest the closing force.
- The handles: single-stranded sequences required to specifically bind to the surfaces, i.e., a magnetic bead on one side and treated glass coverslip on the other.

They are created using dsDNA molecules obtained through either direct synthesis of gene fragments for small hairpins (typically 100 bps), or PCR amplification for larger hairpins of  $\geq 200$  bases. The construction of the hairpin has been extensively described in [Ruiz-Gutierrez et al., 2022]. Here, we focus on the insertion of the G4 motifs.

### 2.1.1 Long DNA hairpin with a G4 embedded

To facilitate the automatic identification of the blockages due to the G4 structures or oligonucleotides, we recommend to work with a DNA molecule containing a long hairpin region of around 1 kb,

as in [Tran et al., 2021], except if you plan to study helicases of lower processivity, for which a smaller hairpin may be more appropriate (as we discuss later). The schematics of a long hairpin is shown in Figure 1-A. The hairpin is formed by closing a dsDNA stretch with a small loop of a few bases (typically 4 to have a timescale of few milliseconds for the spontaneous closure of the hairpin). The other end of the double-stranded hairpin region is ligated to two pre-hybridized oligonucleotides. These oligonucleotides contain 30-bases regions that are complementary to each other and two non complementary region. Once hybridized, they form a Y-shape molecule which contain two non-complementary single-stranded DNA handles. They allow the attachment to both the surface and the magnetic bead. One of these handles is complementary to half of an adaptor oligonucleotide (OliAdaptor). The other half of OliAdaptor is itself complementary to a 50 bases DNA oligonucleotide coating the glass surface - typically attached through click chemistry. The other handle of the hairpin molecule is modified with a double biotin in order to attach to streptavidin-coated magnetic beads. The protocol has been described in detail in [Ruiz-Gutierrez et al., 2022].

To introduce a G4 motif in the hairpin, the 1kb dsDNA region can be modified through standard modification techniques then amplified by PCR. However, if one wants to study the effect of specific epigenetic modifications to the G4 (by the introduction of oxoguanines instead of guanines for example), the G4 motif cannot be amplified. In that case, one must use synthesized oligonucleotides and insert them through ligation in the middle of the pre-digested hairpin region. The construction protocol thus becomes a 5-pieces ligation: the loop, the Y-shape, two dsDNA region resulting from the digestion of the 1kb dsDNA forming the hairpin, and the prehybridized inserts containing the G4 and possible epigenetic modification (Figure 1-A). Non-specific ligations can, in that case, pose a problem, leading to reversed inversion or the insertion of multiple fragments. This can create several blockages that are difficult to identify. They will typically appear in the single-molecule experiments as additional blockages which are not expected, either due to repeated G4 motifs or to mismatches in the ligated overhangs. To avoid that, we recommend to follow some tips (see notes at the end of this paragraph)

#### **Materials**

- Plasmid PS005
- Oligonucleotides with the described sequences.
- BamHI, EcoRI and BsmBI restriction enzymes.
- T4 Ligase and 10X T4 DNA ligase buffer.
- Agarose gels and gel extraction kits
- PCR cleanup kit
- Chemically competent E coli cells (DH5 $\alpha$ , XL10 or equivalent)

#### **Procedure**

1. Cloning of G4forming sequence in plasmid PS005 (see supplementary information for details on the plasmid)
  - Digest 1  $\mu$ g of PS005 by 1U of each EcoRI and BamHI restriction enzymes in 1X CutSmart buffer for one hour at 37°C.
  - Gel purify the digested plasmid band of 3807 bp using an agarose gel DNA purification kit, elute in 10-30  $\mu$ L.

- Anneal equimolar ratio of G-strand and C-strand oligos (for example to form the cMYC G4, the primers cMYC\_Pu27f and cMYC\_Pu27r can be used (Table 1)) by mixing 100 pmol of each oligonucleotide in 100  $\mu$ l Tris 10 mM pH 8.0, 1 mM EDTA buffer and place tube on a dry bath set to 95°C. Remove dry bath from heater and let it cool on a bench until it has reached room temperature. Spin the tube briefly to collect all condensation. Add 1/10 volume of 10x Cutsmart buffer and add 1 U of each EcoRI and BamHI restriction enzyme. Digest for one hour at 37°C. Clean up using a PCR cleanup kit and elute in 30  $\mu$ l ddH<sub>2</sub>O.
  - Ligate 100 nM of the digested plasmid and 2  $\mu$ M of the digested annealed oligo with T4 DNA ligase in 20 $\mu$ L T4 DNA ligase buffer containing 1 mM ATP, for one hour at 25°C or overnight at 16°C.
  - Transform 2  $\mu$ L of the ligation into chemically competent E coli cells.
  - Screen transformed bacteria on LB plates containing 100  $\mu$ g/mL ampiciline isolate recombinant clone containing the desired inserted sequence by colony PCR[Bergkessel and Guthrie, ] or restriction digest of the purified recombinant plasmid.
2. Digest 1 $\mu$ g of the plasmid containing the G4 sequence with 1U BsmBI restriction enzyme in a total volume of 50  $\mu$ L of 1X NEB3.1 buffer at 37°C for one hour.
  3. Migrate the reaction on 1% agarose gel containing EtBr and gel purify the digested plasmid band of  $\sim$  1kbp.
  4. Anneal the Y-shape molecule: Anneal equimolar ratio of PS866 and Treble oligos (Table 2) by mixing 100 pmol of each oligonucleotide in 100  $\mu$ l Tris 10 mM pH 8.0, 1 mM EDTA buffer, and place tube on a dry bath set to 95°C. Remove dry bath from heater and let it cool on a bench until it has reached room temperature. Spin the tube briefly to collect all condensation.
  5. Hairpin ligation step (see Table 1): Mix on ice 15 $\mu$ L of the gel purified plasmid digested by BsmBI, 1 $\mu$ L of the op PS124 oligo (at 10 $\mu$ M) , 1 $\mu$ L of the annealed Y-shape structure, 2  $\mu$ L of the T4 10X DNA ligase buffer and 1  $\mu$ L T4 DNA ligase (400U/ $\mu$ L) 1 $\mu$ L. Incubate at 16°C overnight.
  6. Purify the ligation product on agarose gel to remove the excess of loop and Y-shape

### Tips

- Synthesized oligonucleotide for the inserts allow you to easily add subsequently synthesized epigenetic modifications.
- Use compatible and specific overhangs which are less probable to create non-targeted ligations. See for example [Potapov et al., 2018].
- BsmBI digestion gives non-palindromic overhangs so it is fine to do 1 step ligation to synthesize the hairpin molecule.
- Ligation of the hairpin at 16°C overnight compared to a rapid ligation at 25°C for a few hours improves yields. However, if spurious ligation products are noticed during the downstream steps of hairpin selection, hairpin ligation at 25°C may help resolving such issue.
- For helicases studies use a surface adaptor ensuring no single-strand remains once hybridized. This prevents the binding of the helicase at that position and subsequent removal of the molecule, as described in [Ruiz-Gutierrez et al., 2022, Tran et al., 2021]

Name	Description	Sequence
PS124	Hairpin loop	GCTT <b>GCACTGAGGCGCGGCCTCTCAGTGC</b>
Treble	Tri-biotinylated 5' end oligonucleotide allowing binding of the hairpin to a streptavidin covered magnetic bead	<i>Biotin</i> ( $\times 3$ )-ATGGTCAAGCATGCCGCTTTTCG GTTCCCGTGTGTCTTTTGGTCTTTCTGG TGCTCTTC
PS866	3'-end oligonucleotide allowing annealing of the hairpin to oligonucleotide PS867	ATTCGAAGAGCACCAGAAAGACCAAA AGACACAAAGGGTCAGTGCTGCAACCCAC TTCCTAATCTGTCACTTCTG
PS867	Bridge oligonucleotide to link PS866 with PS625	GTGTCTTTTGGTCTTTCTGGTGCTCTTCG AATCA GAAGATGACAGATTAGGAAGTGG
PS625	sequence containing a 3' DBCO group which covalently binds to the azide coated cover slip	ATTCGAAGAGCACCAGAAAGACCAAAAAGA CACAGACAGATATCGCGCTTCCTCCTACT TTGAATGCTAT- <i>DBCO</i>
Blocking oligonucleotide	7 bp blocking oligonucleotide	GCCGCGC

Table 1: Some DNA sequences used for the  $\sim$  1kbp hairpin. Identical colors are complementary.

### 2.1.2 Small DNA hairpins with a G4 sequence embedded

When we need to study low-processivity helicases, we use smaller DNA hairpin of around 100bp to guarantee complete translocation of the helicase along our molecule before it detaching. This small size hairpins can be simply built by direct ligation of phosphorylated oligonucleotides containing the sequence of interest and a sequence binding to the DNA coating the surface. All our helicase experiments described in this paper were performed in a 87 bp hairpin. Our short hairpin region incorporates the 26 bp c-Myc G4 oncogene promoter sequence (c-Myc Pu27) sequence about 37 bases from the handles (Figure 1-B to -D). They were also intentionally designed with a 7-base single-stranded region (poly-dT) between the OliDBCO-complementary area and the hairpin section. This specific loading-pad segment was dedicated for the binding of a helicase, such as Pif1 [Muellner and Schmidt, 2020, Boulé et al., 2005, Boulé and Zakian, 2006, Boulé and Zakian, 2007, Koc et al., 2016], to the substrate. Limiting the single-stranded region to this short sequence ensures the binding of only one helicase, preventing multiple helicases from binding simultaneously. If the helicase that you study needs a larger loading site, you should adapt that length. Additionally, this region represents the sole available site within the hairpin for binding. In cases where longer hairpins are utilized, and multiple single-stranded regions are present, the binding may occur at various positions, reducing the selectivity and then making more difficult the interpretation of the experiments.

#### Materials

- Synthesized phosphorylated oligonucleotides (see table 2)
  - DNA oligonucleotides Oli-Myc-fwd and Oli-Myc-fwd-comp.
  - Oli-loop



Oligo name	Sequence specificity	Sequence
Oli-Myc-fwd	cMYC-Pu27 G4 in 5'-fwd	GTCTTCTTCTGTCTAATCCTTCACCG TGTCTTTTGGTCTTTCTGGTGCTCTTC- GAA <b>TTTTTTT</b> GCAACTGTCACGATTG ACATAGCATGATAA <b>GGGGAGGGTGGGGAGGGTGGGG</b> AAG- GATCGTACGTACAGCATC
Oli-Myc-rev	cMYC-Pu27 G4 in 5'-rev	<b>aagc</b> GATGCTGTACGTACGATCCTT <b>CCCCACCCTCCCCACCCTC-</b> <b>CCCTTATCATGCTATGTCAATCGTGA</b> CAGTTGC <b>TTTTTTT</b> ACCGGCGCTATTA CCTTCCATAACCAGCTGGCAACATCCAT- CATGATCCGCTACTCCA
Oli-Myc-fwd-comp	cMYC-Pu27 G4 in 3'fwd	GTCTTCTTCTGTCTAATCCTTCACCGT GTCTTTTGGTCTTTCTGGTGCTCTTC- GAA <b>TTTTTTT</b> GCAACTGTCACGATTG ACATAGCATGATAC- CTT <b>CCCCACCCTCCCCACCCTCCCC</b> TATC GTACGTACAGCATC
Oli-Myc-rev-comp	cMYC-Pu27 G4 in 3'-rev	<b>aagc</b> GATGCTGTACGTACGATA <b>GGGGAGGGTGGGGAGGGTGGGG</b> AAGG TATCATGCTATGTCAATCGTGACA GTTGCT <b>TTTTTTT</b> ACCGGCGCTATTAGC TCCATAACCAGCTGGCAACATCCATCAT- GATCCGCTACTCCA
Oli-loop	loop	<b>gctt</b> GCACTGAGAg <b>gcggcc</b> TCTCAGTGC
Oli-Yshape	Yshape	TGGGAGTAGCGGATCATGATGGATGTTG CCAGCTGGTATGGAAGCTAATAGCGC- CGGT
Oli-DBCO	DBCO	ATTCTGAAGAGCACCAGAAAGACCAAAG ACACGGTGAAGGATTAGACAGAAGAA- GAC

Table 2: DNA oligos for short hairpin constructs with cMyc G4. In red the sequences involved in the G4 sequences, in olive the loop apex sequence in blue the sequences involved in loop oligos hybridization before the ligation. In green the polyT sequences used as landing pads for the helicases.

- H<sub>2</sub>O
- T4 DNA Ligase
- ATP solution (10 mM)

### Protocol

1. Annealing of 2 oligonucleotides:
  - Combine 10 $\mu$ l of Oli-Myc-fwd and Oli-Myc-fwd-comp at 100 $\mu$ M + 58  $\mu$ l hybridization buffer . Total volume of 100  $\mu$ l.
  - Heat for 5 min at 95°C and cool down slowly for 1-2h to 25°C in order to allow correct hybridization
2. Ligation of the loop : 10 $\mu$ l of Oli-Myc-fwd/Oli-Myc-fwd-comp-phosphorylated + 10  $\mu$ L Oli-loop-phosphorylated + 5  $\mu$ L T4 DNA ligase Buffer 10X + 1  $\mu$ L T4 DNA ligase + 24  $\mu$ L H<sub>2</sub>O
3. Incubate for 1h at room temperature or at 16°C for 15h + 65°C for 10 min + at 10°C
4. Gel purification using 2% agarose
5. Gel extraction and PCR clean-up

## 2.2 Bead preparation

Here we aim to tether the small DNA hairpin assay to the streptavidin-coated bead through a dual-biotin labeled oligonucleotide that is complementary to the 3' ssDNA handle.

### Materials

- Dynabeads MyOne T1 (Thermofisher).
- Non-biotinylated Hairpin (100 nM).
- Passivation buffer 1X (PB) (140 mM NaCl, 3 mM KCl, 10 mM Na<sub>2</sub>HPO<sub>4</sub>, 1.76 mM KH<sub>2</sub>PO<sub>4</sub>, 2% BSA, 2% Pluronic F-127, 5 mM EDTA, 10 mM NaN<sub>3</sub> pH 7.4).
- Biotinylated bead adaptor (OliBiotin, 100 nM, chemically synthesized, IDT)

### Protocol

1. Dilute both the hairpin resulting from the ligation above and the OliBiotin bead adaptor to a concentration of 40 nM
2. Heat the hairpin at 95°C then let cool down rapidly by diving the tube ice-cold water. This is to avoid cross-hybridization of several hairpins together.
3. Mix 1 $\mu$ L of DNA with 1 $\mu$ L of adaptor with 6 $\mu$ L of PB.
4. The resulting solution of about 5 nM of final concentration is incubated for 30-60 minutes, for hybridization.
5. Dilute the mix 25 times or 100 times

6. Wash  $5\mu\text{L}$  of beads three times with  $200\mu\text{L}$  of PB.
7. Resuspend the beads in  $19\mu\text{L}$  of PB.
8. Take  $2\mu\text{L}$  of the mix (25 times dilution from step 5) +  $5\mu\text{L}$  cleaned beads +  $13\mu\text{L}$  of PB, for a total of  $20\mu\text{L}$  of the solution.
9. Incubate for 20 minutes in rotation at room temperature.
10. Wash three times with  $200\mu\text{L}$  of PB in order to remove unbound NA.
11. Resuspend in  $20\mu\text{L}$  of PB (final concentration of DNA of 0.03 nM to 0.006 nM).
12. Stock beads on a rotator (10 rpm) at room temperature. They can be stored for weeks.

### Tips

- The concentration of DNA and the adaptor before hybridization must be similar, but this and the incubation time may need to be adjusted. If they are too high bead attachment to the surface occurred by multiple molecules, preventing the observation of hairpin openings around 15 to 20 pN, this is the indication that the beads have more than one NA tethered. Thus, in step 4 you can try 100x dilution, and mix then with the beads. If, on the contrary, low attachment indicates insufficient hairpin tethering to the beads, and the concentration of the DNA + OliBiotin can be increased before mixing it with the beads.
- Step 9 in the protocol is crucial to ensure that DNA hairpin + adaptors that did not attach to a bead are not free to bind to the surface and saturate it.
- The above concentrations are the result of the following balance: high concentrations favor the hybridization of the hairpin with OliBiotin. Low concentrations avoid cross-hybridization of the hairpins.

## 2.3 Single-molecule measurements : the stability and folding rate of G-quadruplexes.

In this study, our focus is on characterizing G4 dynamics through magnetic tweezers experiments. Magnetic tweezers function as force clamps, in which for a given magnet position, the magnets apply a constant force to the studied molecules while their molecular extensions ( $\delta z$ ) in nanometers are measured.

To induce G-quadruplex folding, we attach hairpins constructed above between a glass surface and a superparamagnetic bead and then perform force cycles, each cycle consisting of a series of increasing and decreasing force ramps. Figure 2-A sketches the response of a hairpin to the following force protocol: all cycles start when the hairpins are closed at a low force of 4 pN (1). The force is slowly increased to 20 pN and maintained at this force for about 5 seconds before decreasing back to low force ( $\approx 11$  pN). When the force reaches  $F=15$  pN (unfolding force) the hairpin spontaneously opens (2), as seen by the abrupt extension rise, and the molecule stays open until the force is decreased to a force lower than 11 pN (refolding force), where the hairpin extension abruptly decreases indicating a re-hybridization (3) and (4). The hysteresis observed between the hairpin opening and refolding is due to the nucleation step required for the refolding. This process indeed starts from a transient closing at the loop apex. Increasing the number of non-complementary bases in the loop is a simple way to increase the hysteresis and to lower the refolding force threshold. This

is a way to favor the G4 folding, however, having a hairpin which is slow in refolding is not very convenient in the micro-manipulation since we often check that our molecules are single hairpin by cycling opening and closing phases that we want as fast as possible. We have used another method to hinder the hairpin refolding which is more versatile: we inject in the flow cell a few nM of a 7 nt oligonucleotide complementary to the apex loop (shown as green segments in Figure 2-B), when the hairpin is stretched open, this oligonucleotide hybridizes with the apex loop hindering the closing of the loop thus preventing the refolding of the hairpin (2). The hairpin is kept open even when the force is decreased to 7 pN (3a). The hybridization of this 7 nt oligonucleotide is limited in time [Ding et al., 2022] thus the hairpin refolds upon the departure of the small oligonucleotide (4a). Leaving the molecule at moderate force during sometimes allows the folding of the G4. Depending on its sequence, a G4 may fold quickly, after a few cycles or at low rates requiring a lot of cycles. The duration of the hybridization of the oligonucleotide is variable, and, to ensure that the oligonucleotide has left, we impose a phase where the force is reduced to 4 pN or lower. If the oligonucleotide is still attached, it will get ejected from the hairpin, allowing it to completely refold (1) [Ding et al., 2022, Tran et al., 2021, Valle-Orero et al., 2022]. In addition, to promote the formation of G4, we introduce in the microfluidic chamber 200  $\mu$ l of KCl buffer, potassium ions being needed to enhance the formation and stability of G4 structures [Bhattacharyya et al., 2016].

Once the G4 is folded its structure introduces a mismatch in the hybridization of the two strands of the hairpin. The sequence complementary with the G4 sequence cannot find anymore their matching partner and remains as a single-stranded bulge. The consequence upon the hairpin structure strongly depends on the force applied to the hairpin. At medium force  $7pN < F < 11pN$ , the hairpin refolds starting from the apex but stops at the G4 position. Thus, the hairpin remains partially open. This situation has a very clear signature in terms of the molecule extension allowing a simple test to determine the existence of a folded G4. If the force is further reduced, the hairpin can fully refold, keeping the G4 folded and a single-stranded bulge. In this situation, the hairpin extension is equal to that of a fully closed hairpin, no direct signature of the G4 may be deduced from the extension measurement. However, most G4s are quite stable and starting from this G4 structure encircled in a double stranded structure, it is possible to reopen the hairpin by increasing the force above 15 pN, the molecule is then fully stretched excepted at the G4 structure thus this molecule is a few nm shorter than the same molecule without a G4 folded (6). Reducing the force but keeping it larger than 7 pN, we observe that the hairpin just partially refolds allowing detecting unambiguously the G4 folded state. The G4 fold engulfed in a double-stranded structure has its stability challenged by the completely re-hybridized double stranded structure.

Figure 3 is a typical magnetic tweezers trace obtained while following our force protocol (in red) which is constantly applied to all our molecules:

#### Materials

- Tris-KCl buffer: G4Pif1 buffer (10 mM Tris-HCl (pH7.5), 100 mM KCl, 3 mM MgCl<sub>2</sub>)
- Oligonucleotide of 7 bases complementary to the loop.

#### Protocol

1. We verify that our hairpins fully open when the force is increased from 4 to 20 pN (1 to 2), and fully close when the force is reduced to 7 pN or lower (3 and 4).
2. We equilibrate the fluid chamber to Tris-KCl buffer from PB by flowing about 200 $\mu$ L, and while maintaining a constant force cycle composed of the following steps: 4 pN (5-10 seconds) - 20 pN (5 seconds) - 7 pN (15 seconds) - 4 pN (10 seconds), Figure 3-red.

3. 2  $\mu\text{L}$  of 1  $\mu\text{M}$  7b-oligonucleotide, complementary to the loop, is added to the inlet containing 198  $\mu\text{L}$  of Tris-KCl buffer, so a total of 10 nM is flown at a constant rate of 5  $\mu\text{L}/\text{min}$  throughout the chamber. It is sufficient to flow about 100  $\mu\text{L}$  of that solution and then stop the flow.
4. If the oligonucleotide attaches to the hairpin loop during the high force cycle, it will prevent the hairpin from closing, and hence when the force is reduced to 7 pN a shortening in the extension of the molecule of about 1/3 is observed (3a). This reduction in extension is due to the elastic response of the open single-stranded molecule.
5. When after some time (here typically 10s) the oligonucleotide spontaneously detaches from the hairpin, the hairpin closes. The closed molecule reaches here a higher elongation than at the lowest force (4a); this difference in molecule extension between a closed hairpin at 7 pN (4 or 4a) and that at 4 pN (1) is due to the elastic response of the single-stranded handles which remain extended after the closing of the hairpin, and can be calculated using the freely jointed chain model.
6. The G4 structure typically forms after a few cycles spent in a single-stranded state at 7 pN. The duration of this phase is tailored to match the characteristic formation time of each G4 structure. Since the sequence was incorporated in the middle of the hairpin, the formation of the G4 is observed as a blockage at 1/2 of the extension difference between the closed and open state of the hairpin(4b).
7. If the oligonucleotide is still present when G4 has formed, the oligonucleotide blockage is observed first, and only when the latter dissociates, the second blockage due to G4 would be detected.
8. After the majority of our probing molecules exhibited the G4 blockage, we remove the oligonucleotide from the fluid chamber by flushing it with approximately 200  $\mu\text{L}$  of fresh Tris-KCl buffer at a constant speed of 5  $\mu\text{L}/\text{min}$ .
9. Gradually, a reduction in the frequency of oligonucleotide blockages is observed, leaving only the blockage caused by the G4 structure visible. At this force, the hairpin cannot fold due to the hindrance caused by the G4, preventing the contact of the complementary strands that constitute the hairpin (4b).
10. Only when the force is further reduced to approximately 4 pN does the hairpin close around the G4 structure. However, this transition does not always occur automatically; sometimes, additional time is required for the hairpin to fully close and encompass (encircle) the G4 structure within it (5b). One should notice that the G4 structure once formed can be very stable and remained intact even upon full closing or opening of the hairpin.

**Tips:**

- While the syringe pump is on, exercise caution not to run out of buffer in the inlet, otherwise air bubbles will be introduced into the system, and the beads might detach.
- To observe the G4 structure through its blockage, it is crucial to avoid adding an excessive amount of oligonucleotide, as it may dominate the blockage signal. Additionally, it is advisable to extend the 7 pN phase slightly beyond the oligonucleotide's dissociation time. This ensures that even after the oligonucleotide dissociates, the G4 blockage remains visible.

- In cases where the formation of a G4 structure is challenging, adjustments can be made to the oligonucleotide length and waiting time to provide more favorable conditions for G4 formation. For instance, one can opt for a longer oligonucleotide, approximately 8 bases in length, and extend the phase duration to 20-40 seconds. Increasing the oligonucleotide length by just one more base significantly enhance the blockage time, typically by an order of magnitude.
- At times, the hairpin may fully close at 7 pN, temporarily hindering the observation of the G4 blockage. However, this does not imply the absence of the G4 structure which can be probed again at the following cycle. That is precisely why we maintained the force cycles for a minimum of 500s.

### 2.3.1 Orientation

Figure 1-C&D provides the schematics of two deliberately designed substrate versions, LagG4 and LeadG4, each tailored to explore distinct scenarios of helicase interaction with the G4 structure. These designs were carefully crafted to facilitate in-depth helicase studies. As shown by Figure 2-C, in the first scenario, the interaction occurs as the helicase initiates the opening of the hairpin during its translocation on the strand (Lagging strand-LagG4). In the second scenario, the collision occurs within the opposite strand, specifically after traversing the loop, thereby inducing the closure of the hairpin behind the translocating helicase (Leading strand-LeadG4). LagG4 substrate contains the G4-motif (in our studies c-MYC-Pu27: GGG-GAG-GGT-GGG-GAG-GGT-GGG-GAA-GG) in the center of the hairpin region, between the 5' extremity and the loop. On the contrary, LeadG4 assay contains the same motif between the loop and the 3' extremity.

## 2.4 Quantitative analysis of folding and unfolding dynamics of G4 structures

From the observation of our extension traces over many different force cycles we can quantify the dynamics of folding and unfolding of the G4 structure. Here we describe the analysis protocol of that quantification. We call folding times  $T_f$  the times spent by the DNA molecules - in the conditions where the G4 can be formed - until we detect its appearance through a blockage at the expected length. The folding rate is the inverse of the average folding time over many experiments  $k_f = \frac{1}{T_f}$ . This rate is a measure of how fast the structure forms. The conditions in which the G4 can form correspond to low forces in the single-stranded state, i.e when the hairpin is blocked by an oligonucleotide at 7 pN Figure 2-B). We do not count the phases spent in the double-stranded state or at very high force in the computation of the folding times since the formation of the G4 there is very unlikely. We call persistence times  $T_p$  the whole time spent between the first detection of the presence of a given G4 through a blockage at the right position and the first detection of the absence of G4. The unfolding rate is the inverse of the average folding time over many experiments  $k_u = \frac{1}{T_p}$ .

### Detailed analysis protocol [Tran et al., 2021]

1. Record multiple events of G4 formation across numerous beads.
2. The experiment can last more than one day, sometimes you will need several thousand force cycles, in particular in the case of very rare G4 (low  $k_f$ ) or very stable G4 (low  $k_u$ ).
3. Analyze the traces and automatically recognize blockages corresponding to the attachment of the oligonucleotide or the formation of the G4.

4. Compute the folding times as the sum of the times spent in favorable conditions (oligonucleotide present, low force, ss) before each G4 is detected (Figure 3-(3a)).
5. Compute all persistence times as the time the G4 structure is present (and hence blockage is observed) until it unfolds (Figure 3-(4b)).
6. The experimental mean folding time ( $\overline{T_f}$ ) of each G4 sequence was obtained by dividing the whole time spent in the unfolded state (the cumulative time of oligonucleotide blockage before a structure is observed), summed over all beads and over the entire acquisition, by the number of times a G4 structure was formed ( $\overline{T_f} = \sum \text{oligonucleotide-blocking time spent in unfolded state} / \text{total number of folded G4}$ ).
7. Similarly, we defined the mean persistence time ( $\overline{T_p}$ ) or mean unfolding time, as the time spent by a molecule in a G4 conformation before the structure unfolded. It is obtained by dividing the whole time spent in the folded state ( $\geq T_{\text{hold}} = 15$  s) by the number of times a G4 is unfolded ( $\overline{T_p} = \sum \text{time spent in folded state } (\geq 15 \text{ s}) / \text{total number of unfolded G4}$ ).
8. We have seen that the distribution of folding ( $T_f$ ) and persistence ( $T_p$ ) times followed in most of the cases an exponential law, suggesting that the folding and unfolding of the G4 occurs in a single step.
9. The relative error made on these estimation is  $\sqrt{N}$ , where N is the number of observed events (respectively unfolding and folding events).
10. The inverse of  $\overline{T_f}$  ( $k_f = 1/\overline{T_f}$ ) is a direct measure of the probability of folding a G4 structure per unit of time spent at 7 pN. Thus, a longer average folding time indicates a smaller folding probability.

### Tips

- Measure about hundred events per G4 to have sufficient statistics. This can last several hours or days.
- The persistence times and folding times may be very sensitive to the true force applied to bead. Carefully calibrate the force applied to your beads as a function of the magnet position [Gosse and Croquette, 2002, Ostrofet et al., 2018, Papini et al., 2019, Yu et al., 2014].
- To avoid a poor reproducibility due to force fluctuations, discard all beads which seem to display a magnetization higher or lower than usual. This can be achieved by performing slow ramp forces at the start of the experiment. Beads for which the hairpin opens at a magnet position which is very different from the average of all beads shall be discarded.
- To be able to consistently compare the properties of different G4, apply the same force cycles to all of them. The measured persistence time can heavily depend on the duration and value of the high force phase, which destabilizes the G4. The measured folding time can heavily depend on the value of the test force.
- Avoid starting repetitive time-consuming measurements before you actually have an idea of a good force protocol which will fit to the dynamic properties of all of the G4 you want to test in your experiments.
- When two successive cycles showed a blockage at the position of the G4, we assumed that it was due to the same structure and that no unfolding and refolding took place during one single hairpin opening phase.

- There is a non-zero probability that a G4 structure unfolds and then refolds during a fraction of the cycle where G4 cannot be observed. It can happen then that we observe two successive blockages at the G4 position that we would consider as a unique structure while in reality, two successive folding and unfolding events happened. This probability depends on the dynamic of the structure and can be calculated. Details on calculation of this probability are given in Supplementary in [Tran et al., 2021].
- This correction above is important. Without it, your analysis can induce a spurious correlation between the measured folding times and persistence times. Indeed, if the folding time is small, the probability to refold in one cycle is high and you will observe long continuous presence of the G4 although they actually correspond to many events of unfolding and refolding. Typically, for folding times which have a value close to the second, your measured persistence time will increase while the folding time decreases, due to this spurious effect.
- If you always observe a G4 blockage, it is possible that its folding rate  $k_f$  is too high ( $\overline{T_f} \ll$  typical time spent in the test force with the oligonucleotide bound to the loop). In that case G4 forms very easily, and the correction above cannot be used. Indeed, the G4 forms too fast to ever be able to capture its unfolding. In that case, you can adjust your force protocol to make  $k_f$  smaller, for example by increasing the test force to 8 or 9 pN.  $k_f$  typically depends exponentially on the force. You can also decrease the time spent in the test force in the single stranded state in each cycle by decreasing the length of the nucleotide. It will then detach rapidly from the hairpin and allow to increase the time resolution for the folding rate.
- If you never observe a G4 blockage, it may still form but be too unstable. In that case you can try to adjust your force protocol to make  $k_u$  smaller, for example by decreasing the duration of the high force.
- To check the effect of the high force on the persistence time, you can vary the duration of the high force phase  $d_H$  and draw  $\overline{T_p}$  as a function of  $d_H$ . It should vary linearly with  $d_H$  and the intercept of the curve at  $d_H = 0$  will allow you to extrapolate the persistence time in the absence of a high force phase.
- In your design, separate well the G4 from the loop of the hairpin (typically put in the middle of the hairpin) to make the automatic detection easier.
- To ensure reproducibility of the persistence times, adjust the low force to verify that the G4 gets always encircled by the hairpin. The encirclement can be verified by checking the length of the molecule at an intermediate short test phase between the low (encircling) force and the high (hairpin opening) force. If during that intermediate short test phase, the molecule recovers the length corresponding to the G4 blockage, it means that the G4 was not encircled. In that case, lower the value of the low force. If on the contrary it does not recover that length, the hairpin is almost surely completely closed around the G4.
- The length of one cycle corresponds to the lower-resolution limit of our assay. Thus, structures that are less stable than one cycle are not included in the calculation of the average  $T_p$ .

### 3 Observation of Helicase activity in a DNA hairpin

When exploring the world of binding proteins like helicases in the context of hairpins, it's important to know that these proteins might require a specific configuration. There needs to be a stretch of a



few individual bases that remain in a single-stranded format and act as a bridge between the part of the molecule that matches up with OliDBCO and the hairpin region. This unique arrangement is crucial to enable the molecule to successfully bind with the substrate. All the helicase experiments described here are based on short DNA hairpins (100 bp) and on the *Sacharomyces cerevisiae* Pif1 helicase, referred to as Pif1 in our previous work [Valle-Orero et al., 2022]. We worked with small hairpins to ensure the full processivity of the helicase along the hairpin. If the biological question requires that the full translocation through a DNA molecule, the hairpin should be smaller than the enzyme's processivity.

### 3.1 Pif1 helicase expression and purification

Here we describe the materials and method to express and purify the nuclear form of *Sacharomyces cerevisiae* Pif1 (amino acids 40–859) in bacteria [Valle-Orero et al., 2022].

#### Materials

- Plasmid expressing pET28b-His tagged nuclear Pif1 (ADDGENE plasmid #65047)
- *Escherichia coli* BL21(DE3)-derivative Rosetta strain (Novagen)
- Luria Bertani (LB, MP Biomedicals) (per liter): 10 g Bacto-tryptone, 5 g yeast extract, 10 g NaCl. Adjust pH to 7.5 with 1 N NaOH. Autoclave.
- Kanamycin sulfate (50mg/mL in H<sub>2</sub>O) and chloramphenicol (34mg/mL in 100% Ethanol)
- Isopropyl  $\beta$ -D-1-thiogalactopyranoside (IPTG): 1 M solution in ddH<sub>2</sub>O. Filter-sterilize and store at -20C in 1 mL aliquots.
- 5 mL HisTrap FF Crude histidine-tagged protein purification columns (Cytiva)
- Bio-Scale Mini CHT Type I Cartridge # 7324322 (Biorad)
- 5/50 GL MonoS cation exchange column (Cytiva)
- Vivaspin 20, 30 kDa cut off (Cytiva), or equivalent
- FPLC chromatography equipment (Akta pure (Cytiva) or equivalent)
- sonicating equipment (Q705 Fisherbrand sonicator or equivalent), equipped with a 19 mm probe

#### Buffers

- Buffer P (20 mM Na<sub>2</sub>HPO<sub>4</sub>/NaH<sub>2</sub>PO<sub>4</sub> buffer, pH 7.5; 500 mM NaCl; 1 mM tris(2-carboxyethyl)phosphine (TCEP); 10% glycerol)
- Buffer P1 (20 mM Na<sub>2</sub>HPO<sub>4</sub>/NaH<sub>2</sub>PO<sub>4</sub> buffer, pH 7.5, 500 mM NaCl, 1 mM (TCEP), 10% glycerol, 200 mM Imidazole )
- Buffer P2 (200 mM Na<sub>2</sub>HPO<sub>4</sub>/NaH<sub>2</sub>PO<sub>4</sub> buffer, pH 7.5, 500 mM NaCl, 1 mM (TCEP), 10% glycerol)
- Buffer S (50 mM HEPES, pH 7.5; 100 mM KCl; 1 mM TCEP; 10% glycerol)
- Buffer S1 (50 mM HEPES, pH 7.5; 1 M KCl; 1 mM TCEP; 10% glycerol)

- Buffer S2 (45 mM HEPES, pH 7.5; 450 mM KCl; 1 mM TCEP; 10% glycerol)

## Procedure

1. Transform the recombinant plasmid into *Escherichia coli* Rosetta BL21(DE3) cells according to the instructions from the manufacturer.
2. Cultivate *E. coli* cells in Luria Broth (LB) media supplemented with 50µg/ml kanamycin and 34µg/mL chloramphenicol, at 37°C with agitation at 200 rpm.
3. Induce protein expression by adding 0.2 mM IPTG when the culture reaches an optical density (OD600) of 0.8.
4. Cool the culture and allow protein expression to proceed for 16 hours at 18°C under agitation.
5. Perform a second induction with an extra 0.2 mM IPTG for an additional 4 hours at 18°C (see note 1).
6. Harvest the bacterial cells by centrifugation at 5000 g during 15-20 min.
7. Resuspend the cell pellet in buffer P (1/100 culture volume or 5 times pellet volume).
8. Lyse the cells by subjecting the suspension to sonication on ice (40% amplitude, pulse 40%, 10 minutes, 2 seconds on/2 seconds off).
9. Clarify the lysate by ultracentrifugation at 30,000 g for 1 hour.
10. Apply the supernatant from the previous step onto the 5 mL HisTrap Crude affinity column at 1 mL/min
11. Wash the column with five column volume (CV) of buffer containing 20 mM imidazole (90%P, 10% P1)
12. Elute the bound protein with a 20–200 mM imidazole gradient (10% to 100% P1 over 20 CV at 1 mL/min)
13. Check eluted fractions by 8% SDS-PAGE and retain fractions containing Pif1 (see Note 2).
14. Load the selected fractions onto the CHT column equilibrated in buffer P at a rate of 0.5 to 1 mL/min.
15. after a washing step of 10 CV in buffer P, elute the protein with a gradient of 0-40% P2 in 20 CV, then 40 to 100% P2 in 5 CV (see Note 3).
16. Check eluted fractions by 8% SDS-PAGE and retain fractions containing Pif1 and dialyze the collected fractions against 1 L buffer S at 4°C.
17. Load the dialyzed fractions onto the MonoS column at 0.5 ml/min equilibrated in buffer S. After a washing step of 10 CV in buffer S, elute the protein with a gradient of 0 to 100% buffer S1 in 20 CV. (100 mM to 1 M KCl).
18. Check eluted fractions by 8% SDS-PAGE and retain fractions containing pure Pif1.

19. Pool the fractions containing pure Pif1, and concentrate them using Vivaspin centrifugal concentrators. Exchange buffer against buffer S2 and operating several concentration/dilution cycles (at least three) in the Vivaspin device. After the last concentration, add 1 volume glycerol 100%, homogenize and store in aliquots of 15  $\mu$ L at  $-80^{\circ}\text{C}$  (final buffer concentration should be: 25 mM HEPES, pH 7.5; 250 mM KCl; 0.6 mM TCEP; 50% glycerol). see Tip 4.

## Notes

1. 1: The second induction with 0.2 mM IPTG after 16 hours is not mandatory. However, in our hand, it results in a higher recombinant protein yield.
2. 2: The His-tagged nuclear form of yeast Pif1 is 95 kDa. However, in our hands, it usually migrates slightly above 100 kDa on a 8% SDS-PAGE.
3. 3: During the gradient elution on the CHT column, Pif1 elutes below 92 mM Phosphate ( $\sim 40\%$  P2)
4. 4:

## 3.2 Force-dependent helicase

In the realm of magnetic tweezers assays, the study of helicases under applied force has been a subject of great interest. Typically, in these assays, a constant force is maintained, usually falling within the range of 6 pN to 12 pN for DNA studies, ensuring the acquisition of high-quality data. Above this upper limit force, the hairpin can spontaneously open, obstructing the observation of helicase-mediated unwinding activity. Conversely, applying lower forces results in inadequate signal-to-noise ratios. Helicases hydrolyze ATP so that they can unwind the hairpin (ds-DNA) by translocating along one strand and moving away the other strand. Two models are proposed on how unwinding and translocation are coupled, either in a passive way (force-dependent activity) or active one (force-independent activity). While passive helicases, may not exhibit any measurable activity at zero force, active helicases though capable of functioning at zero force, can still be influenced by the applied force [Manosas et al., 2010]. This force plays a role in lowering the height of the activation barrier. Consequently, the observed activity in these assays may not always align with a helicase's behavior as measured in bulk assays. In our previous work [Valle-Orero et al., 2022], we studied Pif1 which is an active helicase. While Pif1 has a high affinity for DNA, it has a lower processivity during the unwinding of the double-stranded DNA [Boulé and Zakian, 2007]. However, it was shown that to enhance its processivity by a factor of 3, from 10 to 31 bp, the force has to increase from 2 to 7.5 pN (at 100  $\mu$ M ATP) [Li et al., 2016]. This insight into Pif1's behavior under force conditions assists in determining of our experimental approach. Given the specific dimensions of our hairpin structure (around 90 bp), we must carefully select a force range that aligns with Pif1's enhanced processivity, and thus we worked between 10-12 pN. This strategic choice ensures that Pif1 can effectively translocate through the hairpin, eventually reaching the G4 structure, all while maintaining its binding and unwinding capabilities without untimely dissociation.

Figure 4-red shows the force protocol designed to track the extension of a hairpin that might contain a formed G4 structure at different forces, and thus the eventual interaction of the helicase with the structure. The first cycle is crucial to determine the formation of G4. For instance, in Figure 4-blue, G4 is absent and the hairpin rezipes completely when the force is lowered from 19 pN to 7 pN. Henceforth, the force is increased to 11 pN and maintained constant throughout the experiment, and the helicase is then injected at a concentration of about 6nM and 1 mM ATP. Pif1 attaches to the single-stranded section of the assay, between the DBCO and the hairpin region, and

moves along the lagging strand in the 5'-to-3' direction, opening the hairpin until it reaches the loop. This is observed by the total extension of the molecule (Figure 4-blue). Subsequently, as Pif1 continues translocating past the hairpin loop along the leading strand, the extension decreases at the same rate. Additionally, we observed instances of the hairpin spontaneously closing, potentially indicating the helicase's dissociation from the ssDNA.

### 3.3 Pif1 unwinding and G4 Resolvase activity

We explored the interplay between Pif1 helicase and a G-quadruplex structure embedded in a small hairpin (87 base pairs) during the unwinding of double-stranded DNA (Figure 5). Once G4s are formed in our probed molecules the structures do not unfold spontaneously during several hours, allowing enough time to test the activity of our Pif1 helicase. Our studies previously published [Valle-Orero et al., 2022], along with earlier evidences [Zhang et al., 2016, Wang et al., 2018, Byrd and Raney, 2015], confirm that Pif1 significantly reduces the lifetime of G4 structures from hours to seconds, and only after Pif1 unfolds G4 can resume translocation.

As described before, two different substrates were used to study the G4 resolvase activity of Pif1 (see Figure 2-C): one in which the G4 motif is located on the translocation strand of Pif1 during unzipping (LagG4) and one in which the G4 motif is located on the translocation strand of Pif1 during the re-zipping of the hairpin (LeadG4). For both substrates, Pif1 displays a pause when it meets the G4. In the LagG4 assay the data shows a single stalling event at the G4 position defined as the resolving time  $\Delta T_R^{LagG4}$ . In the LeadG4 assay, the opposite strand is in close vicinity to then enzyme becoming available, and so the stalling time of the helicase before switching to the opposite strand is less than a second. At this point, the helicase enters in a cyclic dynamic between stalling at the G4 and strand switching, which is concluded when the structure is finally unfolded. Here, the resolving time  $\Delta T_R^{LeadG4}$  is the sum of all the stalling times, where Pif1 is in contact with G4. We have shown that the resolving times for both assays follow a single exponential distribution with a characteristic time of tens of seconds. Also, the kinetics of Pif1 unwinding and rewinding the dsDNA hairpin can be assessed by monitoring the bead's position, following the method outlined in [Li et al., 2016]. To undergo these analyses, we apply a force protocol that enables the observation of our hairpin extensions in the presence of the G4 structure, along with the helicase's interaction with the structure.

#### Materials

- Tris-KCl (G4Pif1) buffer (10 mM Tris-HCl (pH 7.5), 100 mM KCl, 3 mM MgCl<sub>2</sub>)
- Pif1 enzyme (600 nM)
- ATP lithium salt (100 mM)

#### Procedure

1. Ensure most of G4 structures are formed within the microfluidic chamber before introducing Pif1
2. Initiate the force cycle protocol by following these steps (Figure 5-red):
  - Increase the force from 4 pN to 19 pN to achieve full hairpin opening.
  - Close the hairpin at 7 pN, observing the blockage at the G4 position.
  - Temporarily elevate the force to 11 pN for a few seconds to measure the extension of the partially closed hairpin, thereby determining the G4's position.

- Reduce the force to 4 pN to facilitate the hairpin’s closure around the embedded G4 (G4 encircling).
  - Raise the force back to 11 pN and maintain this force during the whole experiment. This force is low enough to maintain the hairpin close, but high enough to enhance the activity of the helicase.
3. Pif1 is added to the microfluidic chamber at a concentration of 6 nM and 1 mM ATP lithium salt (Roche) in G4-Pif1 buffer. Hence, 2  $\mu$ l of 600 nM Pif1 + 2  $\mu$ l (100 mM ATP) is added to 196  $\mu$ l of G4-Pif1 buffer
  4. A flow of 5  $\mu$ l/min of this Pif1/ATP mix is maintained constant.

#### Notes

- Pif1 force range, around 10-12 pN to ensure a processivity of full hairpin. Benefit to work with small hairpins as well.
- When working with a very stable G4 you can wait a long time to ensure that as many hairpins have formed the G4 before injecting your Pif1. However, exercise caution not to wait excessively when working with less stable G4 structures, as they may spontaneously unfold before injection. Strike a balance between the waiting time before injection and the proportion of G4 structures formed on your hairpin molecules
- Consider the buffer composition, selecting one that promotes G4 formation (Na, K) while also being essential for helicase activity (Mg).

#### 3.3.1 Pif1 unwinds the double-stranded hairpin

Pif1 binds to the 7-base single-stranded DNA region within the hairpin assay designed according to the size of the helicase of study. Once it attaches, it initiates translocation along the lagging strand, moving from 5’ to 3’, passing through the loop, and advancing onto the leading strand (Figure 4-blue). In the absence of a preformed G4 structure, this translocation proceeds unhindered. Consequently, the helicase progressively unfolds the hairpin at a consistent rate, as indicated by the continuous extension of the molecule. As Pif1 continues uniformly its movement beyond the loop, the hairpin re-zips, and the initial shortening of the molecule is recovered.

As we showed in Figure 2-C, we have devised two distinct hairpin assays, each featuring the G4 motif situated either on the lagging or leading strand (see also Figure 1C&D). Consequently, we are enabled to investigate the helicase’s behavior in scenarios that mimic situations where the G4 structure lies between the enzyme and the fork (lagging) or when the enzyme is positioned between the fork and the G4 (leading).

#### 3.3.2 Pif1 interacts with G4 in the lagging strand

When G4 structures have formed within the majority of our DNA hairpins, and the process of helicase injection has commenced, we can observe the interaction between these two elements. As shown in Figure 5, the enzyme Pif1 diligently unwinds the double-stranded DNA hairpin (1), which is observed by a gradual increase in the hairpin length (unfolding) until it encounters the G4 structure (2). At this juncture, the progression of the helicase is impeded by the structural hindrance, rendering it unable to continue its translocation, (helicase stalling [Ruiz-Gutierrez et al., 2022]). This impediment manifests as a distinct pause occurring precisely at the G4 position (about 45 bp). This pause (2) persists until the helicase successfully unfolds the G4 structure, at which point it can

resume its translocation along the hairpin (3) and the total elongation of the molecule is observed (90 bp). It bypasses the loop onto the opposite strand driven the closing of the hairpin behind it (4).

### 3.3.3 Pif1 interacts with G4 in the leading strand

In the LeadG4 assay the G4 structure can only form in the leading strand which is where the sequence has been incorporated. In Figure 6-A, our molecule contains the G4 structure, observed as a blockage. It is only then that the force is set to 11 pN and Pif1 is injected into the fluid chamber. After about 10 s, the helicase attaches to the hairpin and starts to translocate through the hairpin causing the partial opening and closing of the hairpin from the G4 position for about 10 s, after which the hairpin fully closes. 400 s later we observe another Pif1 binding and moving through the hairpin, unfolding and refolding the full hairpin without being stalled. Figure 6-B and C) shows the schematics of the hairpin showing key positions of Pif1 when interacts with the G4, and a characteristic magnetic tweezer trace illustrating this steps respectively. After Pif1 has been injected, it binds and unwinds the hairpin all the way to the loop (1 to 3), as observed by a total extension of the molecule, without any stalling along the lagging strand. As the helicase moves pass the loop, the hairpin starts to hybridize behind it, and it only encounters the G4 structure subsequent to its translocation onto the leading strand, positioning itself at the fork just as it collides with the G4. As anticipated, Pif1 translocation through the loop is observed as the full opening of the hairpin (3), succeeded by the partial closure of the hairpin as the helicase walks onto the opposite DNA strand (4b). Then, the helicase continues until it reaches the G4 structure, position at which it is stalled (5). In this assay, the helicase is situated near the opposing DNA strand and strand-switching becomes favored ((5) to (2) repeatedly). After repeatedly unwinding and rewinding the hairpin, Pif1 eventually resolves G4 and continues translocation towards the bead, allowing for the hairpin to fully close (1). We have coined this phenomenon as a "strand switching mechanism": When Pif1 encounters a stall due to the G4 structure, it can, with a high probability, switch to the opposite strand and continue translocating in the opposite direction. Upon successfully traversing the G4 position, we observe, as in the case of LagG4, that the G4 structure has been resolved, as evidenced by the complete closure of the hairpin without the characteristic blockage at the G4 site.

In the LagG4 configuration, the force is preventing the interaction of Pif1 with the opposite strand during G4 stalling by keeping the strands apart, as shown with a cross in Figure 5-B. The transition is still possible but with a very low probability since the transition onto the other strand will require a jump of about 4 nm, compared to a jump of  $\sim 1$  Å in the leading assay.

### 3.3.4 Pif1 resolves G4 [Valle-Orero et al., 2022]

When the helicase resumes its translocation along the same DNA strand after being stall at the G4 position, it suggests that the G4 structure has been successfully resolved. This hypothesis gains further support when the absence of any impediment during the re-zipping of the hairpin confirms that the G4 structure has indeed been unfolded and does not re-form once Pif1 has passed it (as observed by a lack of blockage on the 2nd peak in Figure 5-A&C for LagG4 and Figure 6-A for LeadG4). Notably, the absence of obstruction serves as a distinctive indicator of G4 resolution: a force as high as 11 pN would prevent the hairpin from wrapping around an intact G4 structure [Tran et al., 2021]. If the G4 structure were still present, the hairpin would remain open, and we would observe an obstruction at the same position as prior to Pif1's action. Another compelling piece of evidence supporting G4 resolution is the absence of any pause at the G4 position during subsequent hairpin reopening by Pif1, a pattern consistent with our observations in the initial passage.

### 3.3.5 Kinetics of Pif1 binding to DNA substrates

Our experiments allow very precise measurements of the resolving time of a G4 structure by a helicase, the translocation speed, and processivity. Our traces show that when Pif1 helicase travels through a hairpin and encounters a G4 structure embedded on, it gets stalled at that characteristic position. This encounter is characterized by a stalling event, a blockage at about 45 bases from the handles where the G4 sequence was introduced. Stalling times  $\Delta t'$  correspond to the duration between the initial and final individual stalling events. The resolving times  $\Delta T_R^{xG4} = \Sigma \Delta t'$  (with x being *Lead* or *Lag* substrates) correspond to the cumulative time the enzyme spends in stalling events before it resolves G4 and bypasses the position. In the LagG4 assay the unwinding traces display a continuous pause at the G4 position, after which Pif1 continues translocation, and thus  $\Delta t' = \Delta T_R^{LagG4}$  (Figure 7-A). However, in the LeadG4 assay,  $\Delta T_R^{LeadG4}$  can be obtained for each molecule by summing all individual stalling times  $\Delta t'$ , before the helicase strand switches (Figure 7-B). Between 50 and 100 resolving times should be measured for both of the substrates in order to get sufficient statistics, and histograms are computed with a bin size of around 7s. The histograms and corresponding errors ( $\sqrt{N}$ , N being the frequency in each bin) are then fitted to single exponential distributions. From the fitting procedure we can obtain the characteristic resolving time rate  $\tau_{LagG4}$  and  $\tau_{LeadG4}$  of C-Myc G4 by Pif1, and their errors (Figure 7-C and -D respectively). Translocation velocities of a helicase can be measured from MT traces during hairpin unzipping (vunz) and re-zipping (vz) by fitting the portion of dsNA unwound with a linear function [Valle-Orero et al., 2022, Ruiz-Gutierrez et al., 2022]. Similarly, the processivity of a helicase can be computed on those traces where stalling events do not interfere in the helicase translocation. This processivity is defined as the number of bases the helicase unzips before it detaches from the molecule. In our traces this is computed by measuring the extension that the helicase translocates in nm multiplied by the conversion factor (90 bp/full extension in nm) before detachment occurs.

#### Procedure

1. Molecule extensions and forces were obtained in real time using our in-house interactive data visualization software called Xvin, developed in C/C++. You can access Xvin at the following link: <https://doi.org/10.5281/zenodo.5120049>.
2. Data acquisition occurred at a frequency of 50 Hz, and data collection was conducted under a constant temperature of 25°C.
3. To interpret the extensions of the hairpins as positions of the helicase along the DNA sequence, extensions in manometers (nm) were converted to base pairs (bp). This is done by measuring the average extension change of the hairpins during unwinding at a force of 11 pN. This measurement represented the distance between the lowest and highest points of a complete unwinding event of the hairpin by Pif1. This distance is then divided by 90 bp (length of the hairpin + loop), yielding the length equivalent to the unwinding of one base pair (bp).
4. All stalling events occurred in close proximity to the G4 position within the sequence (approximately  $50 \pm 5$  bases).
5. Stalling times ( $\Delta t'$ ) were recorded, representing the duration between the initiation and conclusion of individual stalling events.
6. Resolving times ( $\Delta T_R^{xG4}$ ) were computed, with 'x' representing either Lead or Lag substrates. These times corresponded to the cumulative time the enzyme is stalled at the G4 position before resuming translocation, providing that blockages at that position are no longer observed, and thus the structure has been properly solved. In the case of the *LagG4*,  $\Delta T_R^{LagG4}$ , is obtained

by considering the continuous time segment at step (2) shown in Figure 5-B. While for the *LeadG4* substrate,  $\Delta T_R^{LeadG4}$  is computed by the sum of individual stalling times ( $\Delta t'$ ) at the G4 position before it resolves the secondary structure, and the hairpin fully recloses.

7. In order to obtain enough statistics on the resolving times, around 50-100 times should be measured for both substrate types.
8. Once those times are recorded, plot them in a histogram with a bin size of approximately 7 seconds.
9. Histograms and their associated errors ( $\sqrt{N}$ , with  $N$  being the frequency in each bin) can be fitted to single exponential distributions. From these fits, you can obtain the characteristic time rates  $\tau_{xG4}$ , and their corresponding error.
10. In the case of the *LeadG4* assay, the individual stalling times ( $\Delta t'$ ) were analyzed in a histogram and fit using a single-exponential distribution from which the characteristic parameter can be obtained. This time is representative of the probability to switch strands.
11. In addition, we can measure both the unzipping and reziping velocities during strand switching transitions. Our previous studies showed very similar values, falling within one standard deviation of approximately  $100 \pm 20$  bp/s. This consistency substantiates that both events are outcomes of the same helicase process.

#### Notes

1. Only molecules that showed an instantaneous unzipping at 19 pN and a complete reziping when the force was lowered to 4 pN, were kept.
2. Once a high percentage of the molecules display the G4 structure, Pif1 is injected. If the G4 structure is very stable you can wait longer, however, be careful not to overpass the persistence time of the G4 under study before injecting Pif1.
3. Once Pif1 has been injected, traces that show stalling events at a position beyond approximately  $50 \pm 5$  bases are discarded since the blockage is considered outside our G4 position (approximately  $50 \pm 5$  bases) and thus, not due to the G4 structure but, for instance, sequence mismatch.
4. When the *LagG4* assay is studied, only traces showing a blockage during unzipping should be considered for analysis. Similarly, traces of the *LeadG4* assay should only show G4 blockages during the reziping of the hairpin.
5. A pause in either unwinding or reziping is identified when the position of the bead remains within a 5 nm window for a duration exceeding 0.3 seconds.
6. Our helicase concentration studies show that increasing the concentration from 6 to 60 nM the frequency of the events increases considerably, while there is no effect in the resolving time of G4.
7. Our traces provide the extension of the hairpin in units of nm. In order to provide these extensions in base pairs units, you need to obtain a conversion factor. In order to do so, we computed a histogram of the hairpin full extensions and fit a Gaussian function, obtaining a mean total extension of 93.0 nm with a standard deviation of 6.1 nm (Supplementary Methods in [Valle-Orero et al., 2022]). In our assay, this average length corresponds to a translocation



of around 90 base pairs. Thus, our conversion factor to convert the position of Pif1 throughout the hairpin from nm to bp, is the ratio 90 bp/93 nm.

## 4 Discussion

The methodologies that we have described in this paper can be used to form, detect and quantify G4 structures in a single molecule DNA hairpin using single-molecule force spectroscopy techniques. The hairpin structure containing a G4 sequence appears as an interesting molecule enabling to access the G4 folded state relatively easily and with a strong signature given by the extension of the hairpin at different forces. Unlike earlier single-molecule assessments conducted under constant forces and not in a double-stranded context [You et al., 2014, Yu et al., 2009, Cheng et al., 2019, You et al., 2015], our assay enables the *in vitro* measurement of G4 folding and persistence times. This capability facilitates the simulation of an environment encountered during the formation of G4 structures *in vivo* such as during replication or transcription. Hence, we have used this method to study the dynamics of different G4 motifs such as human telomeres, human oncogene promoters of cMYC and cKIT genes, and a chicken replication origin [Tran et al., 2021]. Moreover, working with a double-stranded template appears very appropriate to study in real-time helicase activity on G4 structures since a change in the extension of the molecule is observed while a helicase translocates along the hairpin. Using in particular magnetic tweezers force-clamp, we are able to monitor the behavior of the *Saccharomyces cerevisiae* Pif1 helicase during the unwinding of a DNA hairpin that incorporates a G4 structure. Building upon methods from our prior research [Tran et al., 2021, Valle-Orero et al., 2022], we established how to stabilize a G4 structure within a DNA hairpin and further investigate how Pif1 behaves in the presence and absence of the G4. Throughout this technique and the appropriate methodology described in this paper, we are able to visualize the helicase’s translocation along the dsDNA hairpin, its temporary stalling at the G4 position in the sequence, and the subsequent resolution of the structure.

Our assay and the methodology described here will be suitable to study how small molecule binders or G4 binding proteins affect G4 folding and unfolding rates, or how the ligand-DNA complex affects motor progression. In addition, this assay should also help answer a longstanding question concerning specificity of helicases regarding specific G4 folds, since we can see directly in real time folding of the G4 and the behavior of motor proteins when they encounter such structure. However, while we foresee the possibility to study the interaction between helicase and polymerases with G4 structures (preliminary data non-published), we understand that due to the relative complexity of the possible G4 states, it might not be easy to determine the timing of the collision with G4 or G4 unfolding. Thus, the use of FRET signals from fluorescent dyes inserted on both sides of G4 might be necessary.

## 5 Funding

National Research Agency [MuSeq, ANR-15-CE12-0015, G4-crash ANR-19-CE11-0021-01]; CNRS; INSERM; Museum National d’Histoire Naturelle; work in the group of V.C. is part of ‘Institut Pierre-Gilles de Gennes’ [‘Investissements d’Avenir’ program ANR-10-IDEX-0001-02 PSL, ANR-10-LABX-31]; Qlife Institute of Convergence (PSL Univesité). Funding for open access charge: ANR. MR is supported by the Human Frontier Science Program (fellowship LT0039/2022-C).

## References

- [Allshire et al., 1989] Allshire, R. C., Dempster, M., and Hastie, N. D. (1989). Human telomeres contain at least three types of G-rich repeat distributed non-randomly. *Nucleic Acids Research*, 17(12):4611–4627.
- [Bergkessel and Guthrie, ] Bergkessel, M. and Guthrie, C. Colony PCR. 529:299–309.
- [Bhattacharyya et al., 2016] Bhattacharyya, D., Mirihana Arachchilage, G., and Basu, S. (2016). Metal Cations in G-Quadruplex Folding and Stability. *Frontiers in Chemistry*, 4:38.
- [Bohálová et al., 2021] Bohálová, N., Dobrovolná, M., Brázda, V., and Bidula, S. (2021). Conservation and over-representation of G-quadruplex sequences in regulatory regions of mitochondrial DNA across distinct taxonomic sub-groups. *Biochimie*, 194:28–34. Publisher: Biochimie.
- [Boulé et al., 2005] Boulé, J.-B., Vega, L. L., and Zakian, V. A. (2005). The yeast Pif1p helicase removes telomerase from telomeric DNA. *Nature*, 438(7064):57–61.
- [Boulé and Zakian, 2006] Boulé, J.-B. and Zakian, V. (2006). Roles of Pif1-like helicases in the maintenance of genomic stability. *Nucleic acids research*, 34(15):4147–53.
- [Boulé and Zakian, 2007] Boulé, J.-B. and Zakian, V. A. (2007). The yeast Pif1p DNA helicase preferentially unwinds RNA DNA substrates. *Nucleic acids research*, 35(17):5809–5818. Edition: 2007/08/28.
- [Bugaut and Balasubramanian, 2012] Bugaut, A. and Balasubramanian, S. (2012). 5'-UTR RNA G-quadruplexes: translation regulation and targeting. *Nucleic acids research*, 40(11):4727–41. Publisher: Oxford University Press.
- [Byrd and Raney, 2015] Byrd, A. K. and Raney, K. D. (2015). A Parallel Quadruplex DNA Is Bound Tightly but Unfolded Slowly by Pif1 Helicase. *Journal of Biological Chemistry*, 290(10):6482–6494. Publisher: J Biol Chem.
- [Capra et al., 2010] Capra, J. A., Paeschke, K., Singh, M., and Zakian, V. A. (2010). G-Quadruplex DNA Sequences Are Evolutionarily Conserved and Associated with Distinct Genomic Features in *Saccharomyces cerevisiae*. *PLOS Computational Biology*, 6(7):e1000861. Publisher: Public Library of Science.
- [Cheng et al., 2019] Cheng, Y., Tang, Q., Li, Y., Zhang, Y., Zhao, C., Yan, J., and You, H. (2019). Folding/unfolding kinetics of G-quadruplexes upstream of the P1 promoter of the human BCL-2 oncogene. *The Journal of Biological Chemistry*, 294(15):5890–5895.
- [Ding et al., 2022] Ding, F., Cocco, S., Raj, S., Manosas, M., Nguyen, T., Spiering, M., Bensimon, D., Allemand, J.-F., and Croquette, V. (2022). Displacement and dissociation of oligonucleotides during DNA hairpin closure under strain. *Nucleic Acids Research*, 50(21):12082–12093.
- [Ding et al., 2012] Ding, F., Manosas, M., Spiering, M. M., Benkovic, S. J., Bensimon, D., Allemand, J.-F., Croquette, V., Allemand, F., and Croquette, V. (2012). Single-molecule mechanical identification and sequencing. *Nature methods*, 9(4):367–72.
- [Fleming et al., 2017] Fleming, A. M., Zhu, J., Ding, Y., and Burrows, C. J. (2017). 8-Oxo-7,8-dihydroguanine in the Context of a Gene Promoter G-Quadruplex Is an On-Off Switch for Transcription. *ACS Chemical Biology*, 12(9).

- [Gabelica et al., 2007] Gabelica, V., Shammel Baker, E., Teulade-Fichou, M.-P., De Pauw, E., and Bowers, M. T. (2007). Stabilization and Structure of Telomeric and c-myc Region Intramolecular G-Quadruplexes: The Role of Central Cations and Small Planar Ligands. *Journal of the American Chemical Society*, 129(4):895–904. Publisher: American Chemical Society.
- [Gosse and Croquette, 2002] Gosse, C. and Croquette, V. (2002). Magnetic Tweezers: Micromanipulation and Force Measurement at the Molecular Level. *Biophysical Journal*, 82(6):3314–3329.
- [Koc et al., 2016] Koc, K. N., Singh, S. P., Stodola, J. L., Burgers, P. M., and Galletto, R. (2016). Pif1 removes a Rap1-dependent barrier to the strand displacement activity of DNA polymerase . *Nucleic acids research*, 44(8):3811–3819. Publisher: Nucleic Acids Res.
- [Lerner and Sale, 2019] Lerner, L. K. and Sale, J. E. (2019). Replication of G Quadruplex DNA. *Genes*, 10(2):95.
- [Li et al., 2016] Li, J.-H., Lin, W.-X., Zhang, B., Nong, D.-G., Ju, H.-P., Ma, J.-B., Xu, C.-H., Ye, F.-F., Xi, X. G., Li, M., Lu, Y., and Dou, S.-X. (2016). Pif1 is a force-regulated helicase. *Nucleic Acids Research*, 44(9):4330–4339.
- [Manosas et al., 2010] Manosas, M., Xi, X. G., Bensimon, D., and Croquette, V. (2010). Active and passive mechanisms of helicases. *Nucleic Acids Research*, 38(16):5518–5526.
- [Mendez-Bermudez et al., 2009] Mendez-Bermudez, A., Hills, M., Pickett, H. A., Phan, A. T., Mergny, J.-L., Riou, J.-F., and Royle, N. J. (2009). Human telomeres that contain (CTAGGG)<sub>n</sub> repeats show replication dependent instability in somatic cells and the male germline. *Nucleic Acids Research*, 37(18):6225–6238.
- [Mendoza et al., 2016] Mendoza, O., Bourdoncle, A., Boulé, J.-B., Brosh, R. M. J., and Mergny, J.-L. (2016). G-quadruplexes and helicases. *Nucleic acids research*, 44(5):1989–2006.
- [Mitra et al., 2019] Mitra, J., Makurath, M. A., Ngo, T. T. M., Troitskaia, A., Chemla, Y. R., and Ha, T. (2019). Extreme mechanical diversity of human telomeric DNA revealed by fluorescence-force spectroscopy. *Proceedings of the National Academy of Sciences*, 116(17):8350–8359. Publisher: Proceedings of the National Academy of Sciences.
- [Muellner and Schmidt, 2020] Muellner, J. and Schmidt, K. H. (2020). Yeast Genome Maintenance by the Multifunctional PIF1 DNA Helicase Family. *Genes*, 11(2):224.
- [Ostrofet et al., 2018] Ostrofet, E., Papini, F. S., and Dulin, D. (2018). Correction-free force calibration for magnetic tweezers experiments. *Scientific Reports*, 8(1):15920. Number: 1 Publisher: Nature Publishing Group.
- [Paeschke et al., 2013] Paeschke, K., Bochman, M. L., Garcia, P. D., Cejka, P., Friedman, K. L., Kowalczykowski, S. C., and Zakian, V. A. (2013). Pif1 family helicases suppress genome instability at G-quadruplex motifs. *Nature*, 497(7450):458–462.
- [Paeschke et al., 2011] Paeschke, K., Capra, J. a., and Zakian, V. a. (2011). DNA replication through G-quadruplex motifs is promoted by the *Saccharomyces cerevisiae* Pif1 DNA helicase. *Cell*, 145(5):678–91. Publisher: Elsevier Inc.
- [Papini et al., 2019] Papini, F. S., Seifert, M., and Dulin, D. (2019). High-yield fabrication of DNA and RNA constructs for single molecule force and torque spectroscopy experiments. *Nucleic Acids Research*, 47(22):e144.

- [Potapov et al., 2018] Potapov, V., Ong, J. L., Kucera, R. B., Langhorst, B. W., Bilotti, K., Pryor, J. M., Cantor, E. J., Canton, B., Knight, T. F., Evans Jr, T. C., et al. (2018). Comprehensive profiling of four base overhang ligation fidelity by t4 dna ligase and application to dna assembly. *ACS synthetic biology*, 7(11):2665–2674.
- [Ribeyre et al., 2009] Ribeyre, C., Lopes, J., Boulé, J.-B., Piazza, A., Guédin, A., Zakian, V. A., Mergny, J.-L., and Nicolas, A. (2009). The yeast Pif1 helicase prevents genomic instability caused by G-quadruplex-forming CEB1 sequences in vivo. *PLoS genetics*, 5(5):e1000475–e1000475. Edition: 2009/05/09.
- [Ruiz-Gutierrez et al., 2022] Ruiz-Gutierrez, N., Rieu, M., Ouellet, J., Allemand, J.-F., Croquette, V., and Le Hir, H. (2022). Novel approaches to study helicases using magnetic tweezers. *Methods in Enzymology*, 673:359–403.
- [Siddiqui-Jain et al., 2002] Siddiqui-Jain, A., Grand, C. L., Bearss, D. J., and Hurley, L. H. (2002). Direct evidence for a G-quadruplex in a promoter region and its targeting with a small molecule to repress c-MYC transcription. *Proceedings of the National Academy of Sciences of the United States of America*, 99(18):11593–8.
- [Tran et al., 2021] Tran, P. L., Rieu, M., Hodeib, S., Joubert, A., Ouellet, J., Alberti, P., Bugaut, A., Allemand, J.-F. J.-F., Boulé, J.-B. J.-B., Croquette, V., Thao Tran, P., Rieu, M., Hodeib, S., Joubert, A., Ouellet, J., Alberti, P., Bugaut, A., Allemand, J.-F. J.-F., Boulé, J.-B. J.-B., and Croquette, V. (2021). Folding and persistence time of intramolecular G-Quadruplexes transiently embedded in a DNA duplex. *bioRxiv*, pages 2021.01.04.425278–2021.01.04.425278. Publisher: Cold Spring Harbor Laboratory.
- [Valle-Orero et al., 2022] Valle-Orero, J., Rieu, M., Tran, P. L. T., Joubert, A., Raj, S., Allemand, J.-F., Croquette, V., and Boulé, J.-B. (2022). Strand switching mechanism of Pif1 helicase induced by its collision with a G-quadruplex embedded in dsDNA.
- [Valton et al., 2014] Valton, A.-L., Hassan-Zadeh, V., Lema, I., Boggetto, N., Alberti, P., Saintomé, C., Riou, J.-F., and Prioleau, M.-N. (2014). G4 motifs affect origin positioning and efficiency in two vertebrate replicators. *The EMBO journal*, 33(7):732–746.
- [Wang et al., 2018] Wang, L., Wang, Q.-M., Wang, Y.-R., Xi, X.-G., and Hou, X.-M. (2018). DNA-unwinding activity of *Saccharomyces cerevisiae* Pif1 is modulated by thermal stability, folding conformation, and loop lengths of G-quadruplex DNA. *The Journal of Biological Chemistry*, 293(48):18504–18513.
- [You et al., 2015] You, H., Wu, J., Shao, F., and Yan, J. (2015). Stability and Kinetics of c-MYC Promoter G-Quadruplexes Studied by Single-Molecule Manipulation. *Journal of the American Chemical Society*, 137(7):2424–2427. Publisher: American Chemical Society.
- [You et al., 2014] You, H., Zeng, X., Xu, Y., Lim, C. J., Efremov, A. K., Phan, A. T., and Yan, J. (2014). Dynamics and stability of polymorphic human telomeric G-quadruplex under tension. *Nucleic Acids Research*, 42(13):8789–8795.
- [Yu et al., 2014] Yu, Z., Dulin, D., Cnossen, J., Köber, M., van Oene, M. M., Ordu, O., Berghuis, B. A., Hensgens, T., Lipfert, J., and Dekker, N. H. (2014). A force calibration standard for magnetic tweezers. *The Review of Scientific Instruments*, 85(12):123114.

- [Yu et al., 2009] Yu, Z., Schonhofs, J. D., Dhakal, S., Bajracharya, R., Hegde, R., Basu, S., and Mao, H. (2009). Ipr g-quadruplexes formed in seconds demonstrate high mechanical stabilities. *Journal of the American Chemical Society*, 131(5):1876–1882. Publisher: American Chemical Society.
- [Zhang et al., 2016] Zhang, B., Wu, W.-Q., Liu, N.-N., Duan, X.-L., Li, M., Dou, S.-X., Hou, X.-M., and Xi, X.-G. (2016). G-quadruplex and G-rich sequence stimulate Pif1p-catalyzed downstream duplex DNA unwinding through reducing waiting time at ss/dsDNA junction. *Nucleic acids research*, 44(17):8385–94.

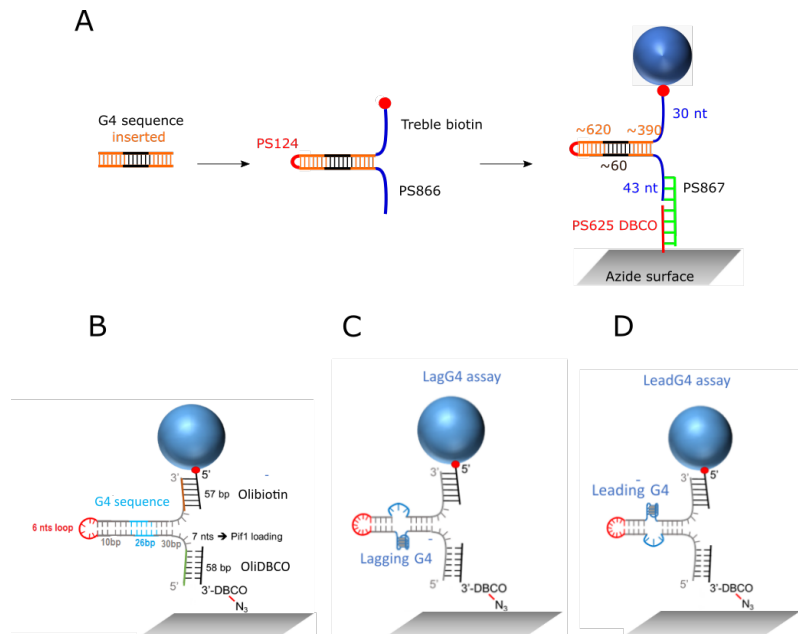


**Figure 1: Hairpin configuration.** **A)** This diagram illustrates the synthesis pathway of a 1kb DNA hairpin that contains a G4 sequence in the center (in black). The dsDNA fragment is ligated on one end to a loop sequence (PS124) and on the other end to a Y-shape molecule formed by annealing DNA oligonucleotide PS866 to the treble oligonucleotide. The DNA hairpin biotin facilitates strong binding to a streptavidin-coated magnetic bead. Tethering to an azide coated glass coverslip is achieved through annealing to oligonucleotide PS867, which is in turn annealed to oligonucleotide PS625. PS625 is covalently linked at its 3' end to the coverslip through a DBCO-azide reaction. **B)** The hairpin construct, spanning 87 base pairs, includes the 26 bp c-Myc G4 oncogene promoter sequence (c-Myc Pu27) positioned in the center of the hairpin (blue). The 5'-end of the hairpin anneals with a 58-base 3'-DBCO modified oligonucleotide (OliDBCO-brown), while the 3'-end anneals with a 57-base oligonucleotide (OliBiotin-green). The 6 nt loop is highlighted in red. The hairpin allows for the loading of a helicase on seven nucleotides that stay single stranded (Pif1 in our case). Two assays were developed: **C)** one featuring the sequence in the strand preceding the loop (LagG4), and **D)** the other following the loop (LeadG4).

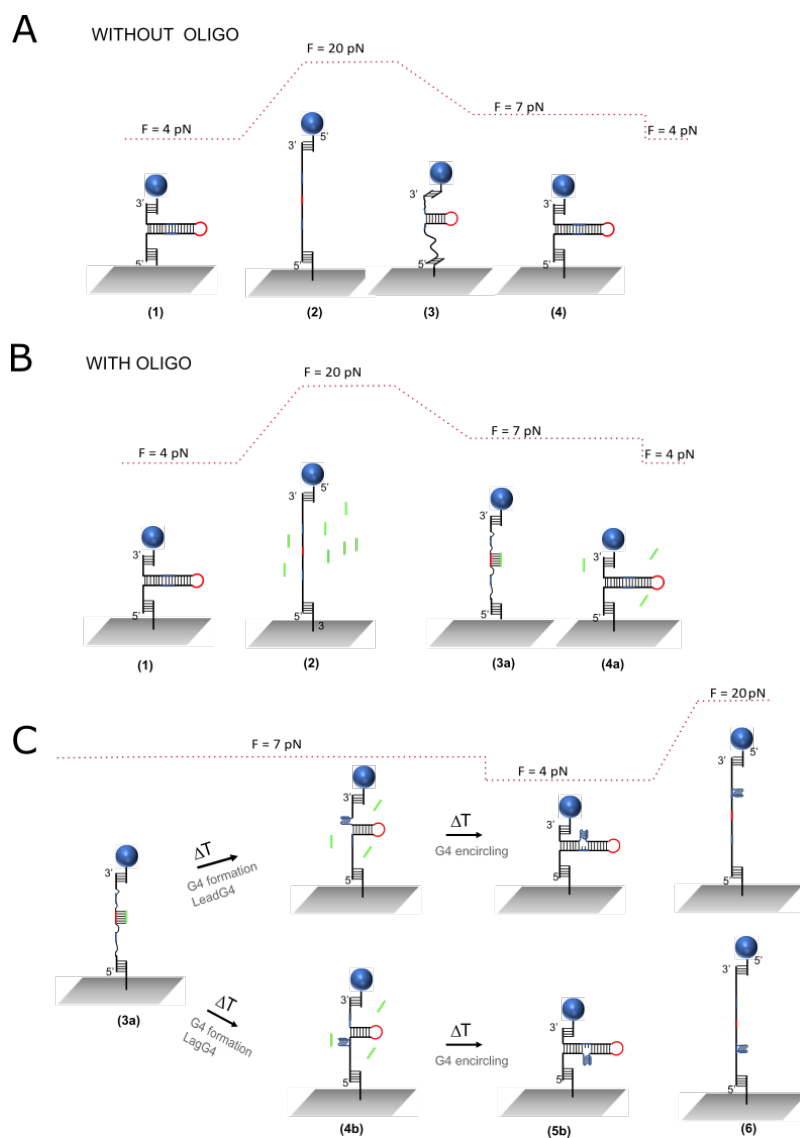


Figure 2: **G4 formation in a hairpin assay.** (A)(B) Sketches of our experiment before and after oligonucleotide injection. Force cycle between 4 pN and 20 pN shows the zippering (1) and rezipping (2) of the hairpin. Partial rezipping(3a) is observed after G4 formation; lowering the force to 4 pN to allow encircling of the G4 structure(4). (C) Sketch of LeadG4 and LagG4 hairpin assays in previously mentioned force cycles. Formation of G4 and lowering the force to zip the hairpin while encircling the G4 structure.

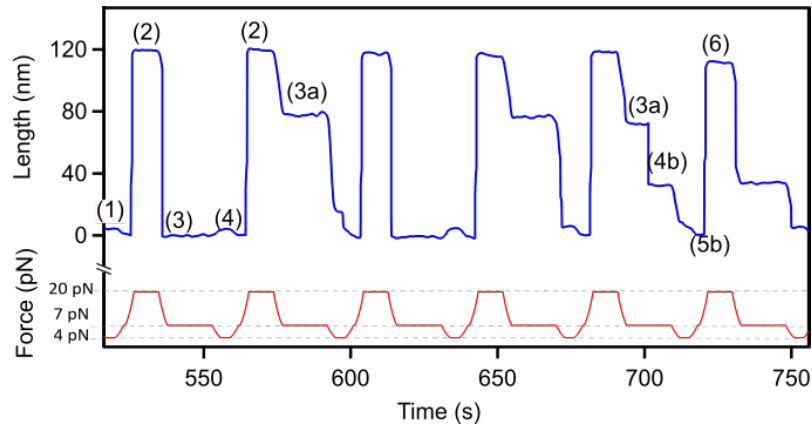


Figure 3: **G4 formation and blockages in the force cycle.** Force extension curve and corresponding extensions. Zipping(1) and unzipping (2) of the hairpin. No blockage is observed before oligonucleotide attachment(4). Blockages observed during rezipping of the hairpin: blockage due to oligonucleotide attachment to the hairpin(3a), G4 structure(4b) and encircling of the G4 structure(5b).

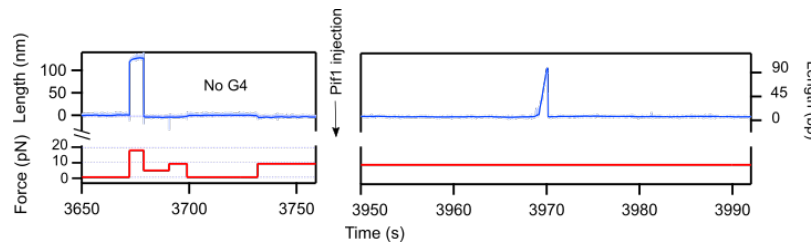


Figure 4: **Pif1 interaction with our hairpin assay where the G4 structure is absent.** Pif1 attaches to a LagG4 hairpin. (Red trace) the force protocol is applied to examine the presence of G4 and its interaction with Pif1. The force remains constant at 11 pN during and after injection of Pif. Pif1 is attached to the DNA (as indicated by the arrow) and moves through the hairpin structure. (Blue trace) the absence of G4 formation is evident as there is no blockage observed when the force is reduced to 7 pN.



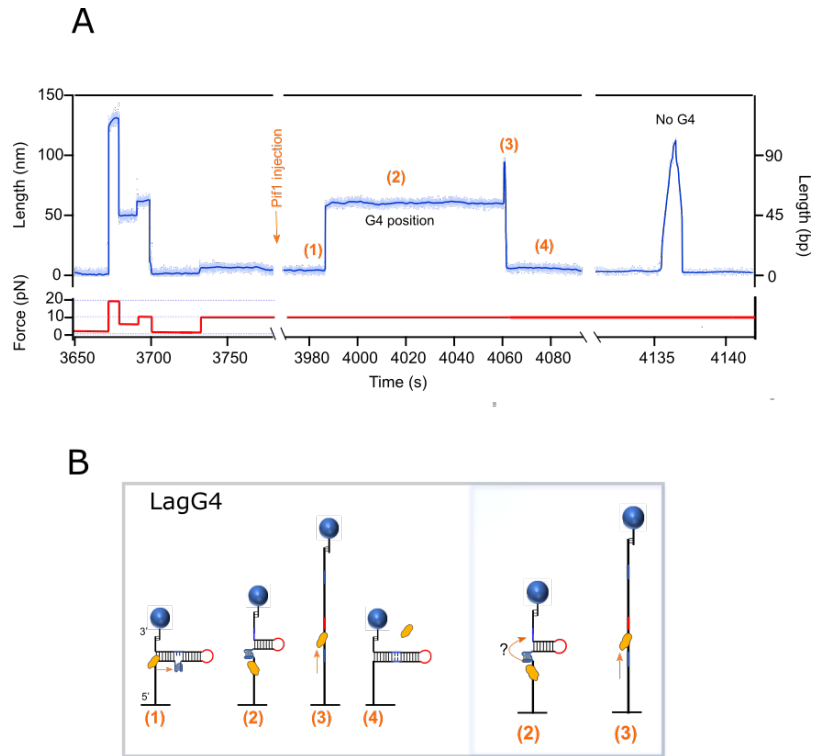


Figure 5: **Pif1 activity on a hairpin with an embedded G4 structure in the lagging strand.** **A)** Magnetic tweezers trace displaying the force protocol in red and the extension curve of the molecule in blue. The force is held steady at 11 pN while Pif1 is introduced and during the measurement. In the first force cycle the extension shows the G4 formation, marked by a blockage at approximately 45 bp. Upon Pif1 injection, it binds to the hairpin (1) and initiates translocation along the hairpin until it encounters the G4 structure, causing it to stall (2). Upon resolving the structure, it resumes translocation through the loop (3), leading to a complete opening of the hairpin (90 bp). It then continues along the leading strand while the hairpin closes behind it (4). A second Pif1 attaches to the hairpin 100 s later, but since G4 is no longer folded, it translocates fully through the hairpin without getting stalled. **B)** Schematic of a hairpin during the interaction of Pif1 with the LagG4 assay which key positions explained in corresponding schematics on B).

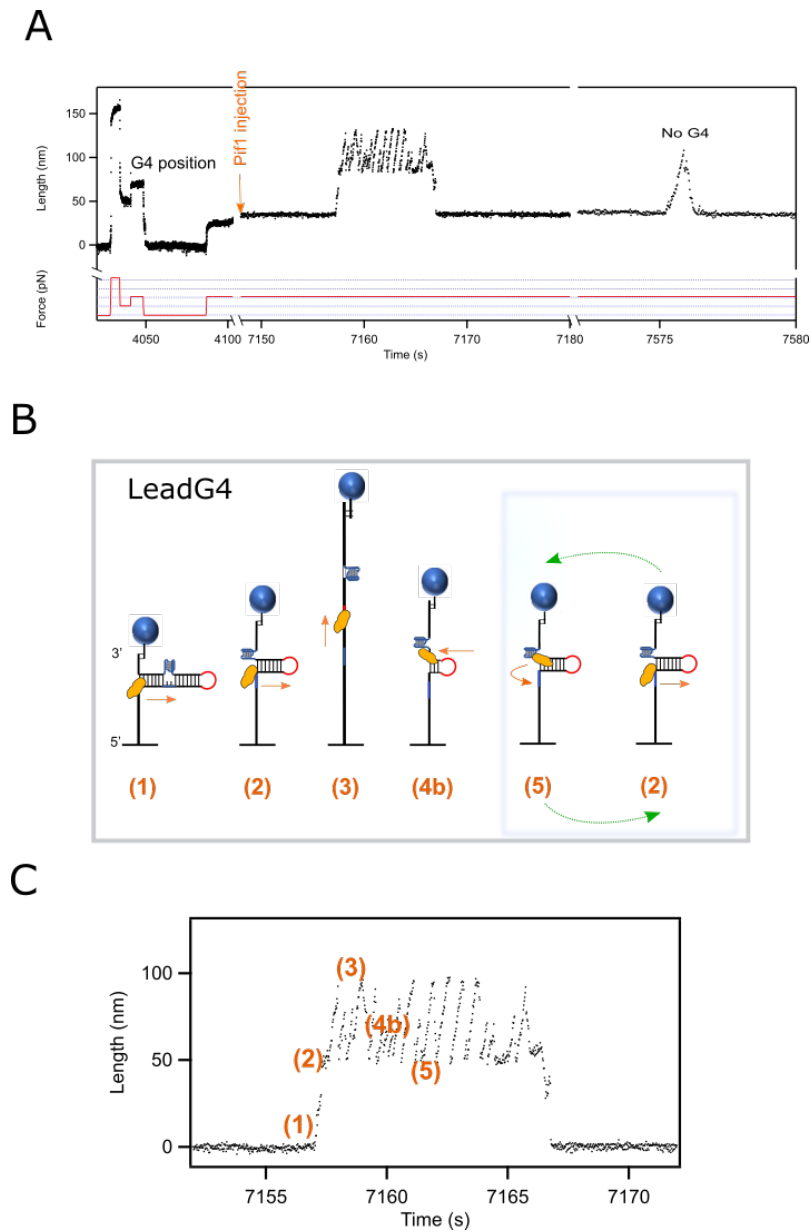


Figure 6: **Pif1 activity on a hairpin with an embedded G4 structure in the leading strand.** **A)** Magnetic tweezers trace displaying the force protocol in red and the extension curve of the molecule in black. Once the force is kept constant at 11 pN, the helicase is injected into the fluid chamber. The trace shows the dynamics of Pif1 when encounters a G4 structure throughout its translocation on the leading strand. This repetitively unfolding and refolding events from the G4 position are described as strand switching. A second helicase translocation more 400 s later shows a continues translocation of Pif1 without a G4 interaction. **B)** Schematic of the hairpin during the interaction of Pif1 with the LeadG4 assay. **C)** This trace demonstrates the interaction between Pif1 and a G4 structure as it moves through a hairpin. Different segments of the hairpin are noticeable as Pif1 travels within it, with key positions illustrated in corresponding schematics on B). In the LeadG4 assay, Pif1 initially progresses through the lagging strand (1-3), passes the loop onto the leading strand (4), and eventually collides with the G4 structure (5). In this collision, the helicase can manage to transition to the other strand with a small jump and begins switching between strands at the G4 position, visiting positions 5 and 2 repeatedly.

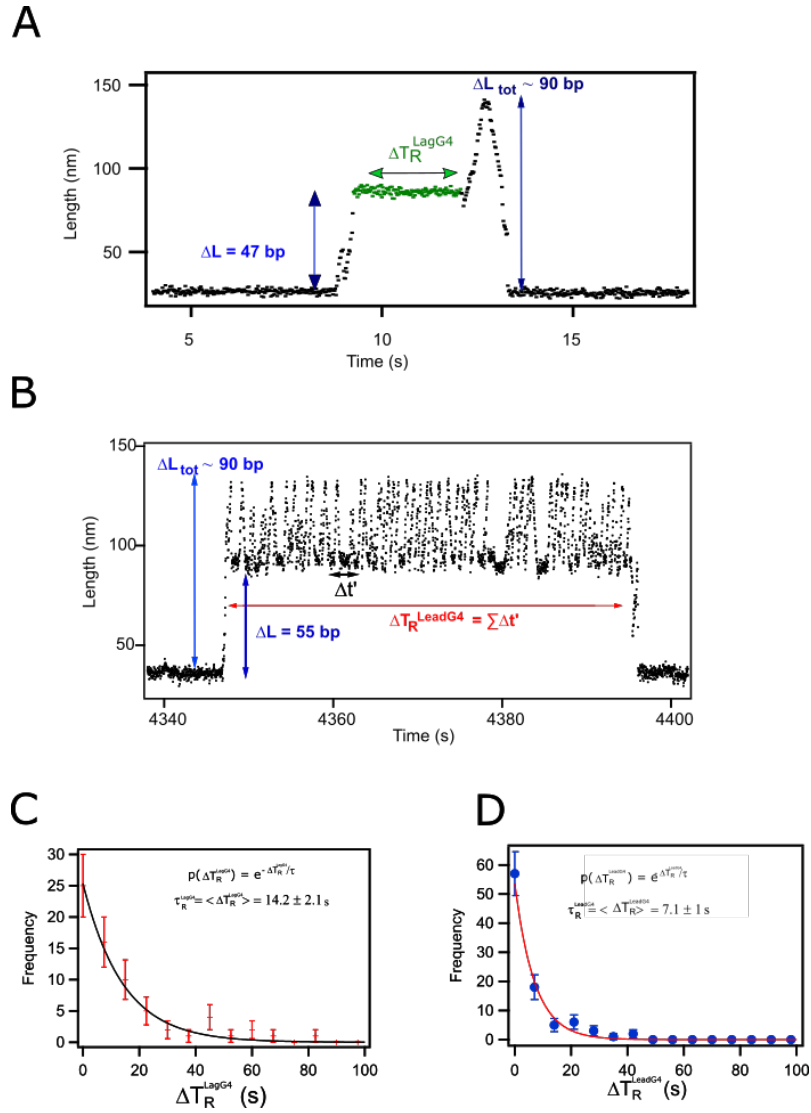


Figure 7: **Data Analysis.** **A)** Pif1 is stalled by the G4 structure before it resolves the structure by a total time of  $\Delta T_R^{LagG4}$  (green). **B)** Here Pif1 is stalled  $\Delta t'$  when in contact with G4, before strands-switching. The sum of all these individual times results in the resolving time  $\Delta T_R^{LeadG4}$  (marked by a red arrow). In both A) and B) the total extension of the molecule is about 90 bp, while the G4 position is at around 50 bp. **C and D)** Distribution of resolving times of G4 show a single exponential with a characteristic time of constant of  $\tau_{LagG4} = 14.2 \pm 2.1$  s and  $\tau_{LeadG4} = 7.1 \pm 1.0$  s for LagG4 and LeadG4 assays respectively